THE JOURNAL OF PHYSICAL CHEMISTRY C

Feature Article

Roles of Phase-Junction in Photocatalysis and Photoelectrocatalysis

Xiuli Wang, and Can Li

J. Phys. Chem. C, **Just Accepted Manuscript** • DOI: 10.1021/acs.jpcc.8b06039 • Publication Date (Web): 29 Aug 2018

Roles of Phase-Junction in Photocatalysis and Photoelectrocatalysis

Xiuli Wang,[a] Can Li[a*]

[a] State Key Laboratory of Catalysis, Dalian Institute of Chemical Physics, Chinese Academy of Sciences, Dalian National Laboratory for Clean Energy, Dalian 116023, China.

[*] E-mail: canli@dicp.ac.cn; Fax: +86 411-84694447; Tel: +86 411-84379070

Abstract

Photo-generated charge separation is one of the key factors determining the solar energy conversion efficiency in photocatalysis and photoelectrocatalysis. Fabrication of phase-junction has been demonstrated to be an effective strategy to construct the internal electric field for the charge separation. Phase junction is essentially a heterojunction, but more common in semiconductor-based photoelectric conversion systems, because most semiconductors exhibit the polymorphous structures. Due to the similar crystal structure between the two phases, phase junctions are more easily formed. The application of phase-junction in photocatalysis and photoelectrocatalysis, especially the anatase-rutile TiO_2 and α-β Ga_2O_3 phase-junction are summarized in this Feature Article. The internal electrical field across the phase junction provides enough driving force for the improved charge separation, evidenced by the time and spatial resolved characterizations. We conclude with a summary and perspectives on the design and application of phase-junction in solar energy conversion systems.

1. Introduction

Artificial photosynthesis, which converts solar energy into chemical energy, is considered as one of the most promising strategies for developing clean and sustainable energy in the future. Storage of solar energy in the form of chemical energy, especially H_2, is proposed to be one of the most ideal approaches, since hydrogen is an excellent energy carrier molecule due to its high specific enthalpy of combustion. Photocatalytic or photoelectrocatalytic (PEC) splitting of water into H_2 and O_2 has been being extensively studied in the past decades.[1-6] Among the factors affecting the photocatalytic performances, light absorption, charge separation and reaction kinetics are the three determining factors. As charge separation is the most complicated and critical factor, it plays the crucial role in the photocatalytic process.

To increase the charge separation efficiency, many strategies have been developed, such as fabrication of junction structure,[7-9] manipulation of facet exposing,[10-12] and loading of cocatalysts.[13-15] Fabrication of heterojunction is regarded as a general strategy to improve charge separation in semiconductors.[8] The phase junction in polymorph semiconductors, which is essentially a heterojunction, has been first proposed based on the considerably increased photocatalytic activities in anatase-rutile phase-junction TiO_2[16]. The phase junction is more common in semiconductor-based photoelectric conversion systems, since semiconductor always have several phase structures. And then the phase junction has been demonstrated as an effective strategy to increase the charge separation and transfer across the different phases.

In this feature article, we begin with a brief review on the progress of applications of the phase junction strategy in both photocatalysis and photoelectrocatalysis, especially TiO_2 and Ga_2O_3 phase

junction. Then we discuss the kinetic mechanism of the phase junction from the viewpoints of time and spatial resolved characterization, mainly focusing on the anatase-rutile TiO_2 phase-junction. We summarize the conclusions and give the perspective remarks of the phase-junction strategy in the field of solar energy conversion.

2. Applications of phase-junction in photocatalysis and photoelectrocatalysis

As the most studied photocatalyst, TiO_2 has been extensively studied with different phase structures, including anatase, brookite, rutile, and TiO_2-B.[17-24] A particular interest is also devoted to the mix-phased TiO_2. In the research of environmental photocatalysis, TiO_2 containing both anatase and rutile phases always show much higher activity than either pure anatase or rutile TiO_2.[25-37] The synergism between anatase and rutile particles was claimed to be the reason for the improved photocatalytic performances. Degussa P25, which is a mixture of rutile and anatase, was always selected to be a model catalyst for its high activity of photocatalytic H_2 production for a long time, although the reason for its good performance is not clear.[5]

For the first time, phase junction was proposed to be the main reason for the improved photocatalytic activity of anatase:rutile TiO_2.[16] Then this strategy is applied to other semiconductor-based photocatalyst systems in both photocatalysis and photoelectrocatalysis. In this section, we first review the work on TiO_2 phase-junction, followed by the work of Ga_2O_3 phase-junction in photocatalytic water splitting. And then, the application of phase-junction in photoelectrocatalysis is summarized, and the relation between the photocatalytic and photoelectrocatalytic performance for the particulate semiconductor-based photoconversion systems with surface phase-junction structure is discussed.

2.1 Roles of TiO_2 phase-junction in photocatalytic H_2 evolution

TiO_2 has been extensively studied to explore its application in photocatalytic water splitting owing to its unique physicochemical properties[24]. Anatase and rutile, with the bandgap of 3.0 and 3.2 eV, are the most widely investigated crystal structure of TiO_2. Anatase usually displays higher activity than rutile in photocatalytic reactions,[38-39] such as photodegradation of environmental pollutants, while rutile is illustrated to be more active for photocatalytic water oxidation and overall water.[40-41] However, as discussed above, the mixed-phase structure TiO_2 (e.g. Degussa P25 TiO_2) containing both anatase and rutile has received much attention, because they always exhibits higher photocatalytic activity than either anatase or rutile alone.

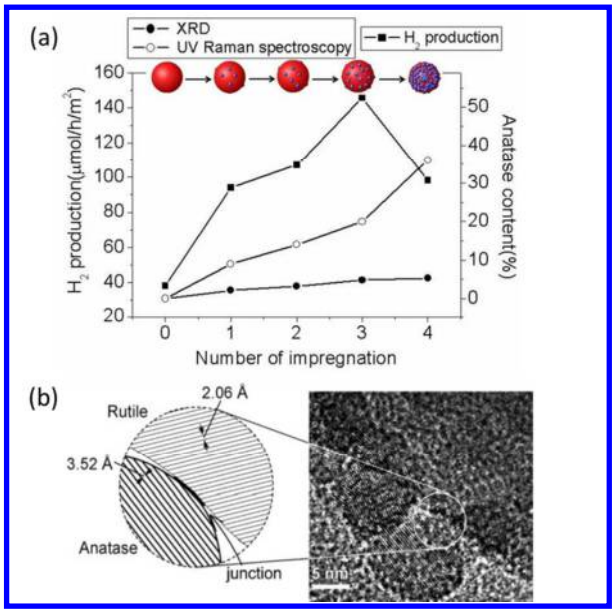

Figure 1. (a) Photocatalytic H_2 evolution of rutile TiO_2 loaded with increasing amount of anatase nanoparticles. (b) HRTEM of the surface phase-junction formed between anatase and rutile. Reprinted with permission from ref. 16. Copyright 2008 Wiley-VCH.

With UV-Raman to characterize the phase structure of the anatase-rutile mixed-phase TiO_2, the effect of mixed-phase structure of TiO_2 on the photocatalytic H_2 evolution reaction was investigated in detail.[16] TiO_2 samples with different anatase-rutile phase-junction were prepared by thermal

treatment of $Ti(OH)_4$ in air from 500 ^oC to 800 ^oC. The phase compositions both in the bulk and surface region were estimated from XRD and UV Raman spectra, respectively. A maximum activity of H_2 is obtained for TiO_2 samples calcined at 700–750 ^oC, where the surface is in a mixed phase of anatase and rutile. When TiO_2 completely transformed into rutile with calcination temperature above 800 ^oC, the photocatalytic activity decreases dramatically. Inspired by these results, the concept of surface phase-junction formed between anatase and rutile TiO_2 was proposed for the first time. To confirm this viewpoint, anatase nanoparticles were deposited onto rutile surface by wet-impregnation method. As shown in Figure 1a, the photocatalytic activity increases with the amount of anatase nanoparticles increasing. However, the activity decreases if anatase is overloaded, because the surface phase-junction exposed on the surface of TiO_2 will be reduced by the overloaded anatase. The perfect phase-junction, clarified by the closely contacted anatase-rutile interface in the HRTEM images (Figure 1b), is proposed to facilitate charge separation at the surface of TiO_2.

Degussa P25, with anatase-rutile mixed-phase structure, is regarded as a benchmark TiO_2 for its high photocatalytic activity. The excellent performance of P25 must result from the synergistic effect between anatase and rutile. The activity can be further improved via an elaborately controlling thermal treatment, which optimize the anatase–rutile phase-junction structure of P25.[42] As shown in Figure 2, the activity of P25 can be enhanced up to 3–5 times in the reactions of photocatalytic reforming of methanol, propanetriol and glucose. Further increasing the thermal treatment temperature does not increase the photocatalytic activity, indicating that the crystallization degree is not the major reason for the considerably enhanced photocatalytic activity of the thermal-treated P25 photocatalysts. Therefore, the optimized anatase-rutile phase-junction obtained from P25 by elaborately controlling thermal treatment mainly contributes to the enhancement of the activity.

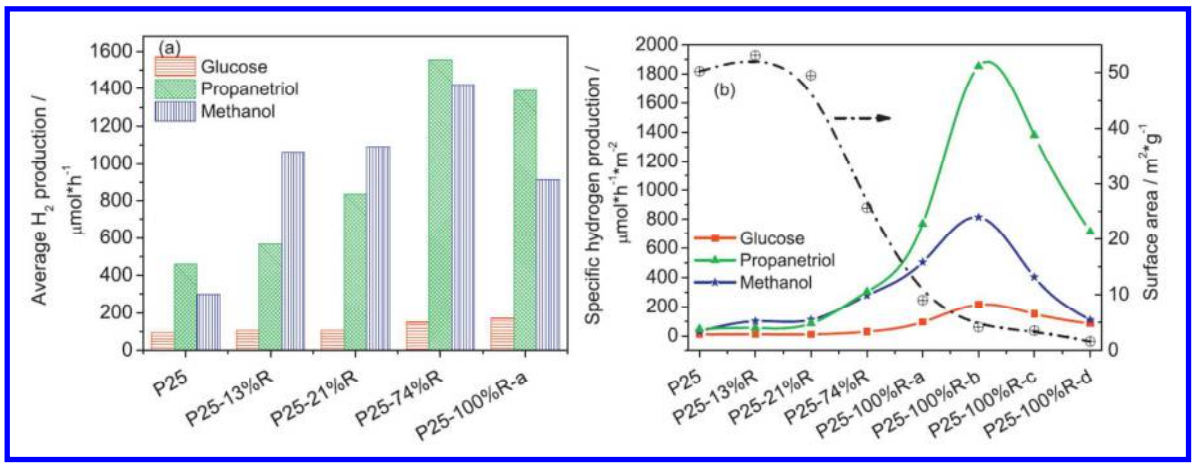

Figure 2. (a) Average H_2 production in photocatalytic reforming of methanol, propanetriol and glucose and (b) surface-specific photocatalytic activity for H_2 evolution in photocatalytic reforming of methanol on Pt/P25-x%R photocatalysts (where x indicates the rutile content estimated by XRD. For P25-100%R-a, b, c, d photocatalysts, where a, b, c and d indicate different treatment conditions), the surface areas of P25-x%R photocatalysts are also displayed (dash dot). Reprinted with the permission from ref. 42. Copyright 2011 Elsevier.

With the realization of the importance of phase-junction, new strategies for controlling phase-junction have attracted more attention. Additives, such as Na_2SO_4, $NaNO_3$, $NaHCO_3$, Na_3PO_4, Na_2SiO_3, and Na_2MoO_4 have been found to have the phase controlling ability[43]. For example, surface modification of Na_2SO_4 is found to restrain the phase transformation of TiO_2 from anatase to rutile.[44] With the amount of SO_4^{2-} increases from 0 to 3 wt%, the anatase percentage in surface region can increase from 2% to 75%. Using this method, TiO_2 with different phase structures can be prepared at the same temperature, and these catalysts are more comparable. As shown in Figure 3, in comparison to P25, the as-prepared TiO_2-SO_4^{2-} shows an increase up to 6-fold for photocatalytic H_2 production via methanol reforming. The characterization of UV Raman spectroscopy and XRD demonstrates that the restrained phase transformation of anatase phase by SO_4^{2-} results in a mixed phase structure

of TiO_2 even after high temperature calcination. The anatase-rutile phase-junction, together with the high crystallinity of TiO_2, contribute to the excellent photocatalytic activity of H_2 production.

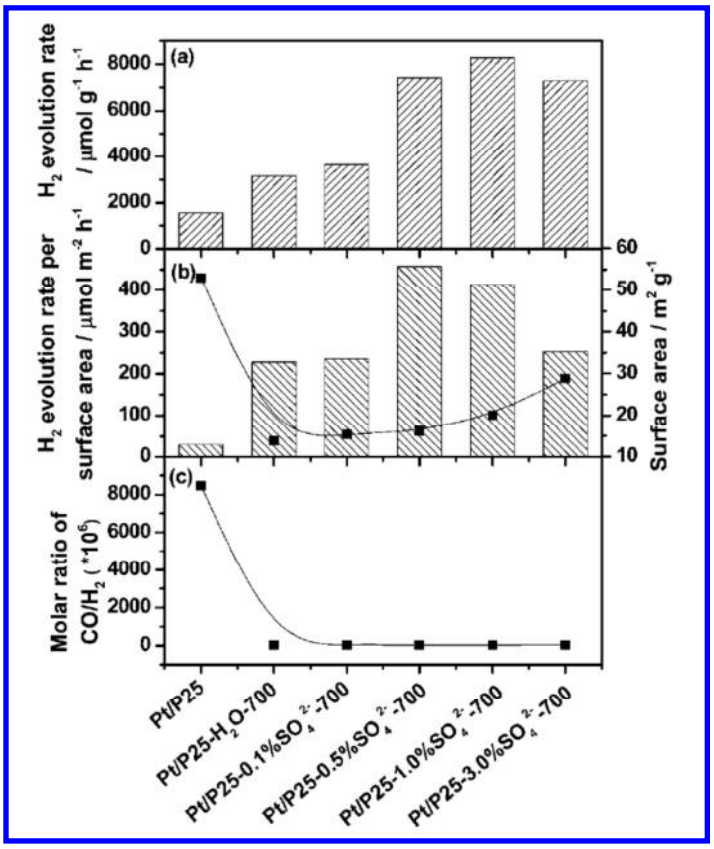

Figure 3. (a) Overall photocatalytic activity of H_2 evolution. Surface-specific photocatalytic activity of H_2 production (b) and CO selectivity (c) of Pt/P25, Pt/P25-H_2O-700 and Pt/P25-x%SO_4^{2-}-700 catalysts. The solid line in (b) indicates the surface area of the samples. Reprinted with the permission from ref. 44. Copyright 2012 Royal Society of Chemistry.

Since the anatase:rutile phase-junction strategy was introduced in photocatalysis, it became a guidance in the preparation of TiO_2 with different morphology, such as nanoparticles[45-46], nanorod arrays[47], and nanobelts[48] structures.[49-53] Besides anatase and rutile phase, other TiO_2 phases can also form phase-junction, which could facilitate the photogenerated charge separation.[54] For example, bicrystalline structure consisting of TiO_2(B) and anatase exhibited a much higher H_2 production

activity as compared to P25.[30, 35] The phase junction fabricated with TiO_2(B) improve the charge separation and enhance the photocatalytic activity.[55-63] Nanotubular anatase/rutile/TiO_2(B) nanostructures with enhanced interfacial charge separation and transportation displays excellent photoactivity for the photocatalytic production of hydrogen.[64]

2.2 Roles of Ga_2O_3 phase-junction in photocatalytic overall water splitting

With the understanding of the TiO_2 phase-junction, the phase-junction strategy is used into the photocatalytic overall water splitting, in which Ga_2O_3 phase-junction is well-studied. There are five polymorph phases of Ga_2O_3. Among them, Ga_2O_3 with four polymorphs (α-, β-, γ-, and ε-Ga_2O_3) has been utilized in the field of catalysis, making it as a good candidate for phase-junction study.[65-71]

The effect of Ga_2O_3 phase-junction was first investigated with α-β phase-junction Ga_2O_3 prepared at elevated temperatures by phase transformation from α-Ga_2O_3 to β-Ga_2O_3 phase.[72] As characterized by XRD and UV Raman spectroscopy, the original α-Ga_2O_3 transforms into β phase upon the calcination temperature increasing from 673 to 1073 K. As shown in Figure 4d, Ga_2O_3 calcined at 863–893 K show much higher activity than the pure phase Ga_2O_3 samples in α (673 to 773 K) or β phase (973 to 1073 K) in photocatalytic overall water splitting.[73] Typically, the photocatalytic activity of Ga_2O_3-863 with surface α-β phase-junction, which is higher than that of the mechanically mixed Ga_2O_3, increases up to three or seven-fold of pure α-Ga_2O_3 or β-Ga_2O_3 alone, respectively. The α–β phase junction contributes to the considerable enhancement in the activity of photocatalytic overall water splitting, as there are no distinct changes in particle size or surface area among these samples. The α-β phase-junction of Ga_2O_3-863 was investigated by high resolution transmission electron microscopy (HRTEM). The images in Figure 4a and 4b demonstrate that the formed β-Ga_2O_3 nanoparticles are sporadically patched on the surface of the large α-Ga_2O_3

particle, resulting in that both α and β phases are exposed on the Ga_2O_3 surface. A simplified cartoon in Figure 4c depicts the α–β phase junctions with a lattice mismatch of only 3%, which promote the charge separation efficiency.

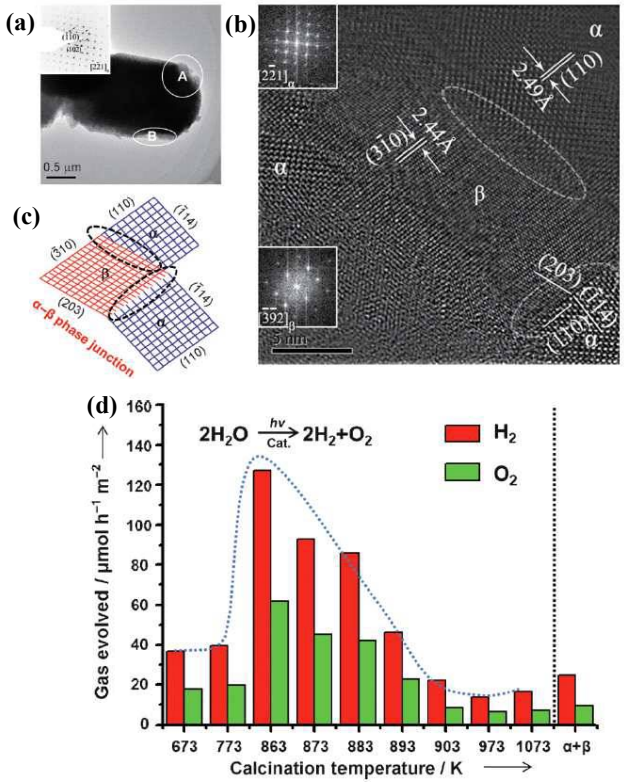

Figure 4. (a) Low-magnification TEM image of Ga_2O_3-863. The inset is the SAED pattern of area A, indicating that area A contains both α and β phases. (b) HRTEM image of area B in (a). (c) A simplified cartoon depicting the α–β phase junctions. (d) Specific H_2 and O_2 evolution activities (normalized by specific surface area) of Ga_2O_3 samples prepared at different temperatures. The notation α+β indicates the mechanically mixed Ga_2O_3 with a 1:1 ratio of α-Ga_2O_3:β-Ga_2O_3. Reprinted with permission from ref. 73. Copyright 2012 Wiley-VCH.

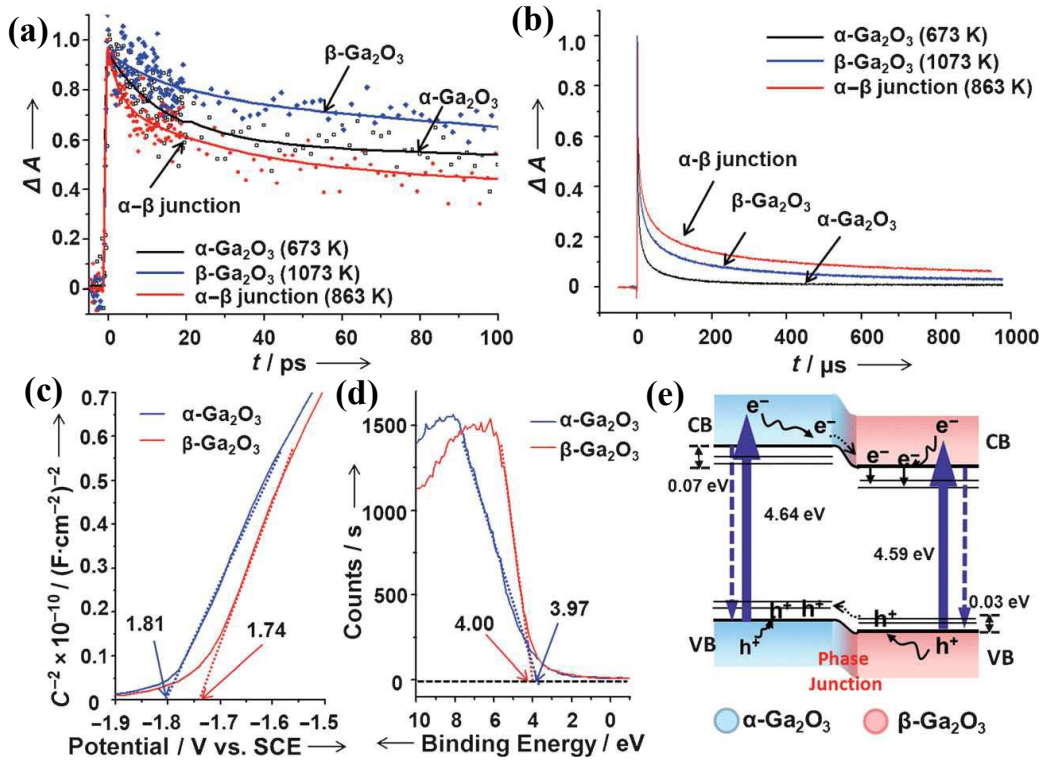

Figure 5. (a) Normalized transient absorption decays at 850 nm of Ga_2O_3 samples excited by a 255 nm laser. (b) Normalized transient absorption decays of average mid-IR absorption of Ga_2O_3 samples excited at 266 nm. Mott–Schottky curves (c) and XPS valence band spectra (d) of α-Ga_2O_3 and β-Ga_2O_3. (e) Illustration of charge transfer across the α–β phase junction. Reprinted with permission from ref. 73. Copyright 2012 Wiley-VCH.

Time-resolved spectroscopy was used to understand the role of α–β Ga_2O_3 phase-junction in the photocatalytic reaction. The Ga_2O_3-863 with α–β phase-junction shows an ultrafast transfer at approximately 3 ps (Figure 5a), which is faster than recombination (>1000 ps) and trap processes (14–32 ps) in Ga_2O_3. On the other hand, for Ga_2O_3-863 with α–β phase-junction, the lifetime of the long-lived electrons is much longer than that in either α-Ga_2O_3 or β-Ga_2O_3 in the microsecond time-scale (Figure 5b). The increased long-lived electrons most likely contribute to the enhancement in the photocatalytic activity.

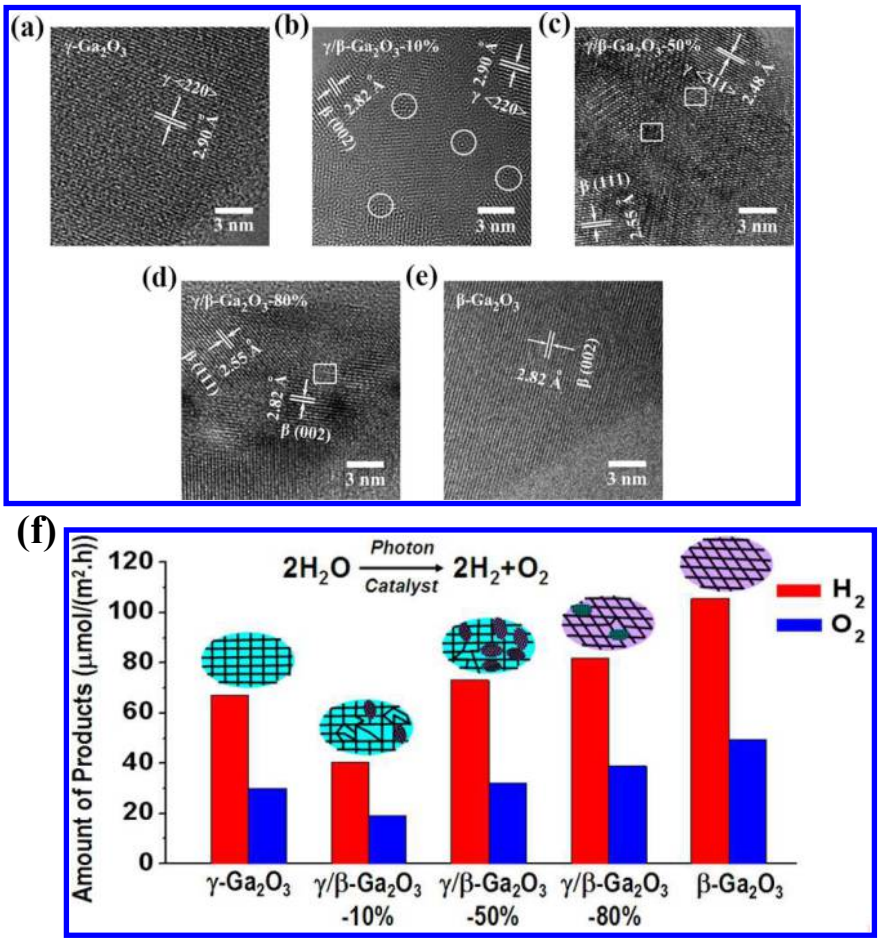

Figure 6. HRTEM images (a-e) of γ-Ga_2O_3, γ/β-Ga_2O_3-10%, γ/β-Ga_2O_3-50%, γ/β-Ga_2O_3-80%, and β-Ga_2O_3 samples (the areas scaled out by circular and square symbols indicate the disordered structure). (f) Photocatalytic overall water splitting activities of Ga_2O_3 photocatalysts. Reprinted with permission from Ref. 74. Copyright (2015) American Chemical Society.

The effect of other Ga_2O_3 phase-junction is also investigated, besides the α–β Ga_2O_3 phase-junction. Ga_2O_3 photocatalysts with γ-β phase-junction was synthesized by calcining γ-Ga_2O_3 at 823 K for different times (0.75, 5, 11, and 24 h) in air.[74] As shown in Figure 6f, all the Ga_2O_3 samples can split water stoichiometrically into H_2 and O_2. However, opposite to that of the α-β phase-junction Ga_2O_3 system, the γ-β phase-junction Ga_2O_3 with a small amount of β phase shows the lowest activity. Characterization of the HRTEM images (Figure 6a-e) shows that much more

disordered structure exists between the γ and β phases in the γ/β-Ga_2O_3-10% photocatalyst due to the defective spinel structure of γ phase. The decrease of photocatalytic activity in the γ/β-Ga_2O_3-10% photocatalyst is because that the disordered structure serves as charge recombination centers, revealed by the spectroscopic characterization and theoretical calculations. Based on the results of α-β and γ-β Ga_2O_3 phase-junction, it is demonstrated that the interfacial structure between two phases is decisive for the efficiency of charge separation. To boost photocatalytic reactions, the structure of the phase-junction should not to be disordered or defective.

2.3 Roles of phase-junction in photoelectrochemical water splitting

On the basis of the application of phase-junction in photocatalysis, its role in photoelectrocatalytic (PEC) reactions is also widely studied.[51, 75-79] The Ga_2O_3 particles with α-β phase-junction and TiO_2 particles with anatase-rutile phase-junction were used in the photoelectrochemical water splitting.[76] The film electrodes were fabricated by electrophoretic deposition in an acetone solution containing Ga_2O_3 or TiO_2 powder. For Ga_2O_3 samples, all the electrodes show increasing photocurrent densities during the potential scanning from −1.2 to 1.2 V versus SCE. The photocurrent density of the β-Ga_2O_3 electrode (Figure 7e) is almost 3 times as high as that of α-Ga_2O_3 electrode (Figure 7a). Opposite to the improved photocatalytic activity by the α-β phase-junction Ga_2O_3, all Ga_2O_3 electrodes with α-β phase-junction show decreased photocurrent density. Among all the electrodes, the Ga_2O_3-863 electrode shows the lowest photocurrent density (Figure 7b). The similar negative effect of phase-junction on PEC performance is observed in TiO_2 electrodes with anatase-rutile phase-junction. The negative effect on PEC performance is mainly due to the increased charge recombination between semiconductor particles by the surface phase-junction, as indicated in Figure 7f. In principle, the phase junction can promote charge separation in the

particle regardless of its application in PC or PEC reactions. But there is severe interfacial charge recombination in the PEC reaction, since the photoexcited charges have to transport across semiconductor particles to reach a conducting substrate or electrode surface.

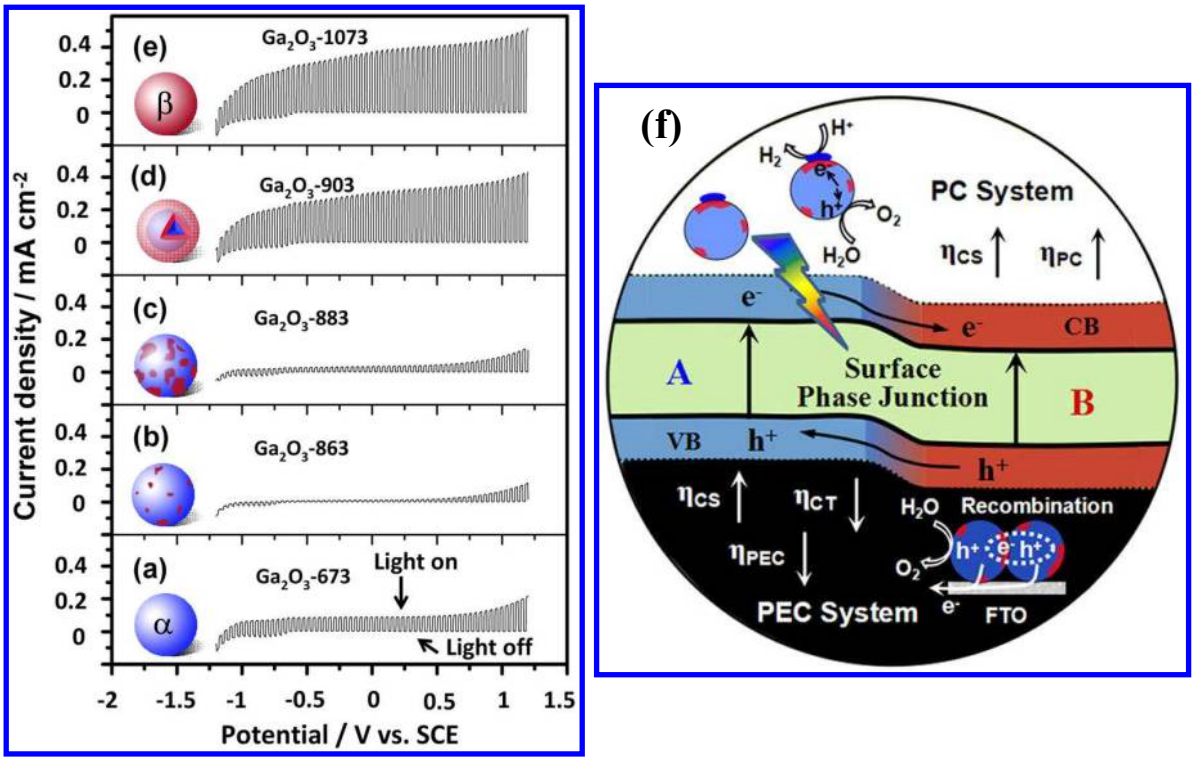

Figure 7. Photocurrent−potential curves (a-e) of the Ga_2O_3 electrodes with α-β phase-junction. The inserted cartoon images indicate the phase composition of Ga_2O_3 samples. The blue and red particle represents α and β phase. (f) A scheme of the role of α-β Ga_2O_3 phase-junction in PC and PEC performance. Reprinted with permission from Ref. 76. Copyright (2015) American Chemical Society.

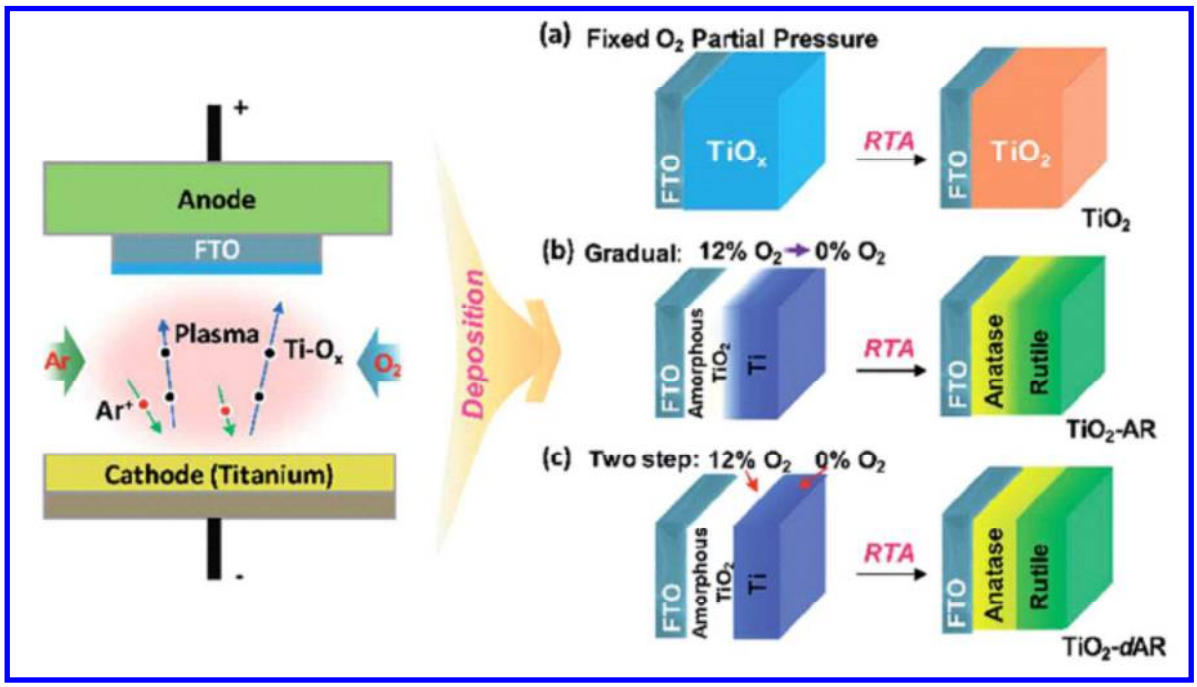

Figure 8. Schematic diagrams of the fabrication strategy for TiO_2 films with tunable phase structures using a direct current reactive magnetron sputtering technique followed by rapid thermal annealing (RTA) treatment. (a) Pure phase films of TiO_2-A and TiO_2-R were prepared by RTA treatment of the precursor films deposited at a fixed O_2 partial pressure of 12% and 0%, respectively. (b) The TiO_2-AR film was prepared by RTA treatment of the precursor film obtained by gradually adjusting the O_2 partial pressure from 12% to 0%. (c) The TiO_2-dAR film was prepared by RTA treatment of the precursor film with an internal and external layer deposited at a fixed O_2 partial pressure of 12% and 0% O_2 partial, respectively. Reprinted with the permission from ref. 77. Copyright 2016 Royal Society of Chemistry.

To utilize the phase junction strategy in PEC, the effects of the phase configuration and interface structure across phase junctions were studied with anatase-rutile TiO_2 films in detail. The anatase-rutile TiO_2 films were fabricated using a direct current reactive magnetron sputtering technique followed by rapid thermal annealing (RTA) treatment (Figure 8). Firstly, the effect of

phase configuration were investigated with three samples, type A, B and C with random phase alignment (deposited at 0.3% O_2), with forward phase alignments (the TiO_2-dAR electrode), and with reverse phase alignments (the TiO_2-RA electrode), respectively. The photocurrent–potential curves of these three TiO_2 electrodes shows that the photocurrent densities are in the order of type B > type A > type C at 0.8 V_{RHE} (Figure 9b). On the other hand, in terms of the effect of the phase-junction on onset potential, the TiO_2 electrode in type B phase alignment configuration exhibits the lowest V_{onset} of ca. 0.15 V_{RHE}, while the TiO_2 electrode in type C and A phase alignment configuration displays the largest onset potential of ca. 0.48 V_{RHE} and a moderate onset potential of ca. 0.27 V_{RHE}, respectively. Secondly, the effect of interface structure of the phase-junction was studied further with the type B phase alignment configuration. As shown in Figure 9c, the TiO_2-AR electrode prepared by gradually adjusting the O_2 partial pressure exhibits a photocurrent density of ca. 0.63 mA cm^{-2} at 1.23 V_{RHE}, which is much higher than 0.15 mA cm^{-2} of the TiO_2-dAR electrode. The photocurrent density of TiO_2-AR electrode is 3 and 9 times those obtained for the TiO_2-A and TiO_2-R electrodes, respectively. Furthermore, the onset potential of TiO_2-AR electrode is negatively shifted to ca. 0.15 V_{RHE}. TiO_2-AR and TiO_2-dAR electrodes show dramatic differences in PEC, although they are in the same anatase/rutile phase alignment (Figure 8b and 8c). Revealed by transient absorption (TA) spectroscopy, TiO_2-AR also shows higher yields of long-lived holes under illumination than that of TiO_2-dAR, indicating that the phase junction prepared by the gradual deposition method facilitates charge separation and transfer (Figure 9d). These results demonstrate that the appropriate phase alignment and interface structure of a phase-junction is vitally important in the utilization of phase-junction in PEC system. This work demonstrates directly the great potential of phase-junction for efficient charge separation in photoelectrochemical water splitting.

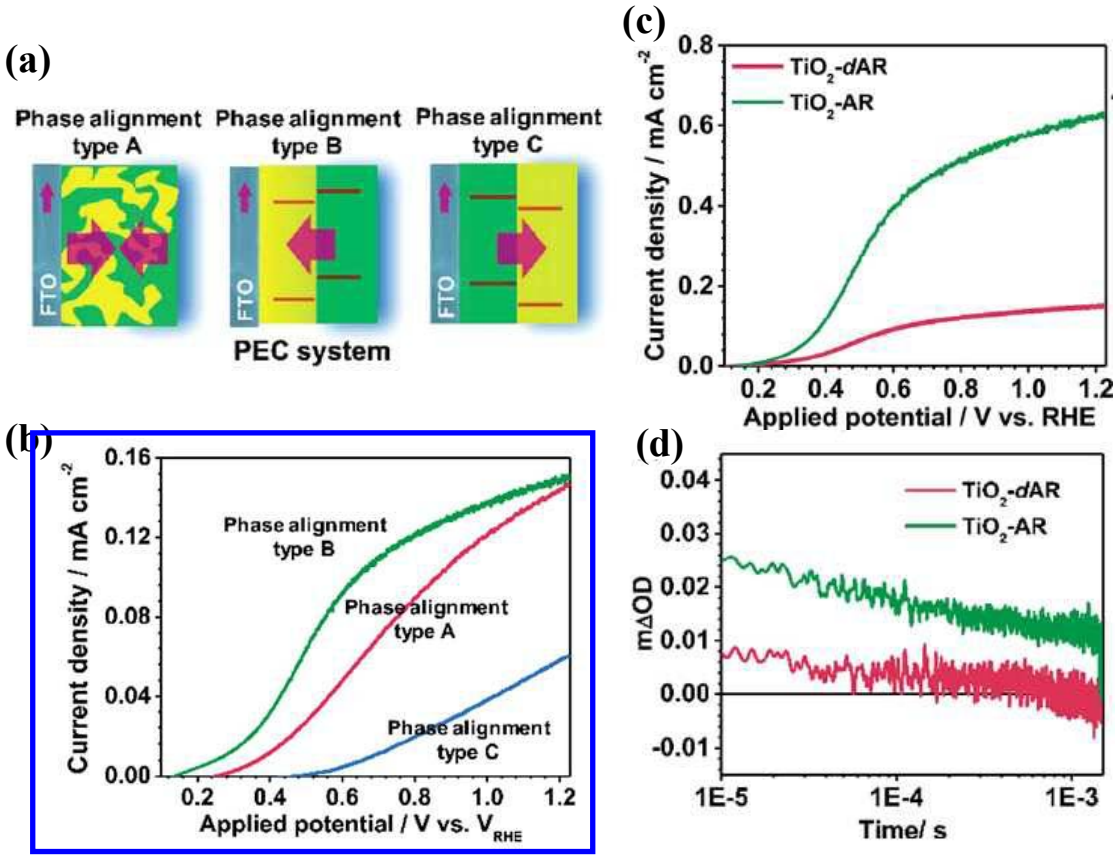

Figure 9. (a) Schematic diagrams showing the different configuration of the anatase-rutile phase-junction. Type A, Type B and type C are the TiO_2 electrodes with random phase alignment (deposited at 0.3% O_2), with forward phase alignments (the TiO_2-dAR electrode), and with reverse phase alignments (the TiO_2-RA electrode), respectively. (b) Photocurrent−potential curves of TiO_2 electrodes with type A (red), type B (green) and type C (blue) phase alignments. Photocurrent−potential curves (c) and transient absorption decay profiles (d) of TiO_2-dAR (red) and TiO_2-AR (green) electrodes. Reprinted with the permission from ref. 77. Copyright 2016 Royal Society of Chemistry.

3. Charge separation promoted by phase-junction

The phase-junction strategy has been successfully applied in both photocatalytic and photoelectrochemical water splitting, as summarized above. The phase-junction can increase charge separation and then prolong charge lifetimes, resulting in the improved photoactivity. To confirm the charge separation, many researchers are devoted to investigate the thermodynamical band alignment both theoretically and experimentally. On the other hand, the charge separation process and the distribution of the long-lived charges are characterized by time and spatial resolved techniques directly.

3.1 Band alignment

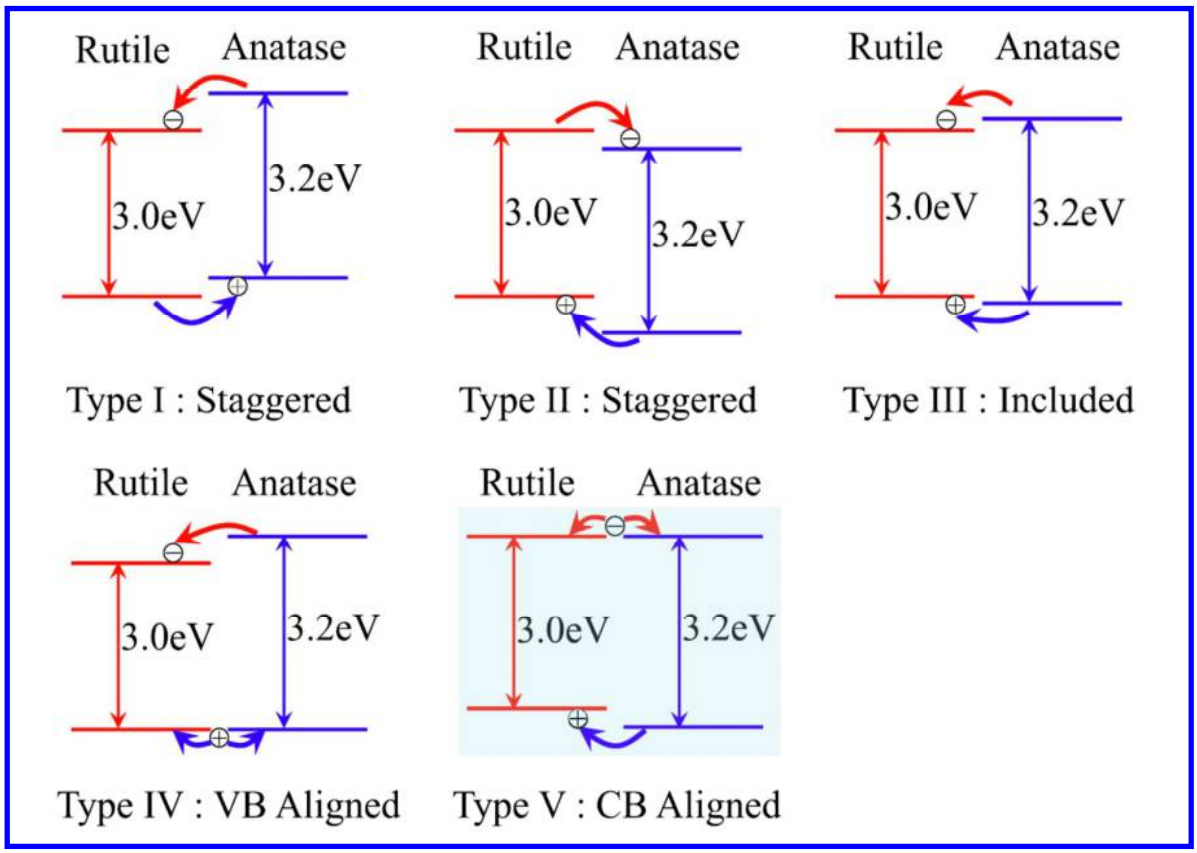

Figure 10. Schematic illustrations of five possible band alignments between rutile and anatase. Reprinted with the permission from ref. 80. Copyright 2015 Nature Publishing Group.

The band alignment between the different phases of the phase-junction determines the interfacial charge transfer directions thermodynamically, then the charge separation efficiencies. The bandgaps of different phases are quite similar due to the same chemical composition, which makes it hard to identify the positions of the conduction bands (CB) and valence bands (VB) of different phases. Moreover, the band alignment is very sensitive to the interfacial structure, the gas atmosphere or the electrolyte, etc. Thus, many researchers devoted to clarify the band alignment theoretically or experimentally.[81-93]

The band alignment between anatase and rutile TiO_2 has been extensively studied. In summary, five possible band alignments of anatase-rutile phase-junction have been proposed for the relative position of CB and VB levels of TiO_2, as shown in Figure 10.[80] The flat band potentials of anatase and rutile single crystals were measured with electrochemical measurements, and it is reported that the flat band potential of anatase is 0.2 eV above that of rutile,[89] indicating the VB are aligned (type IV in Figure 10). The type IV band alignment, with higher CB of anatase and similar VB of anatase and rutile, is also supported by the calculation results of Kang et al[82] and experimental results.[94-95] The work function of the valence band was studied by the photoemission measurement, and it is found that the work function of rutile VB is 0.2 eV lower than that of anatase,[88] demonstrating that the CB are aligned (type V in Figure 10). The staggered band alignment, which promotes charge separation efficiently, is also proposed.[93] The first staggered type is with both of the CB and VB of anatase above those of rutile (type I in Figure 10),[86] and conversely the second type is with both of the CB and VB of rutile above those of anatase (type II in Figure 10).[81, 83-84] Scanlon et al.[84] proposed the type II staggered band alignment from theoretical calculations, and they further performed X-ray photoemission spectroscopy (XPS) measurement of nanoparticulate structured

rutile-anatase bilayer, demonstrating the type II band alignment of 0.4 eV exists between anatase and rutile with rutile possessing the higher conduction band minimum, as shown in Figure 11. The included alignment (type III in Figure 10)[96] was also proposed based on the characterization results of electron paramagnetic resonance (EPR) spectroscopy.

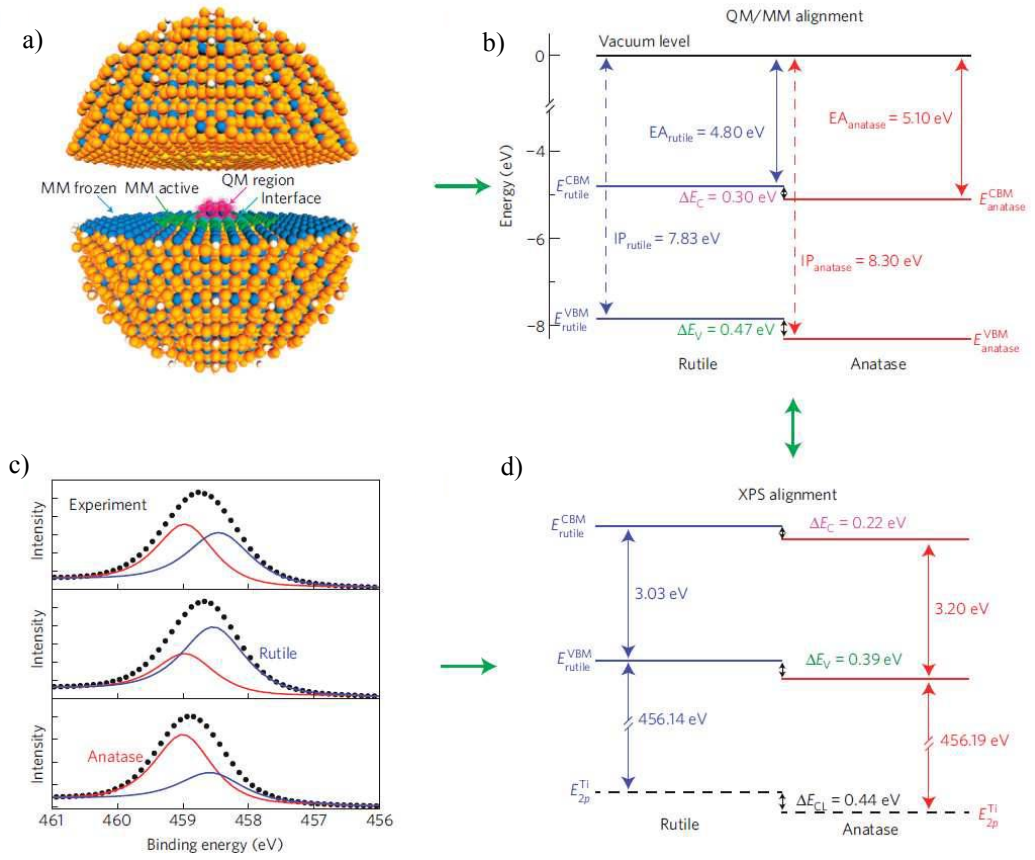

Figure 11. Band alignment of anatase-rutile phase-junction from XPS and QM/MM. (a) Graphic of the hybrid QM/MM cluster used for rutile in the positive charge state. (b) Schematic illustration of the QM/MM alignment of rutile and anatase TiO_2. (c) Ti $2p_{3/2}$ spectra taken from phase-junction composite particles with rutile to anatase ratios of 1:1 (top) and 2:1 (middle) and 1:2 (bottom). (d) Schematic illustration of the XPS alignment between rutile and anatase. Reprinted with the permission from ref. 84. Copyright 2013 Nature Publishing Group.

In the theoretical calculation on the atomic structure of anatase/rutile phase-junction, a set of novel theoretical methods were used by Liu et al.[91, 97-99] They proposed an ordered three-phase junction, a layer-by-layer "T-shaped" anatase/TiO_2-II/rutile junction. Although the intermediate TiO_2-II phase is only a few atomic layers thick, it is critical to alleviate the interfacial strain of anatase/rutile junction. The three-phase junction is claimed to be a single-way valve allowing the photoinduced charge transfer but frustrating the charge flow in the opposite direction.

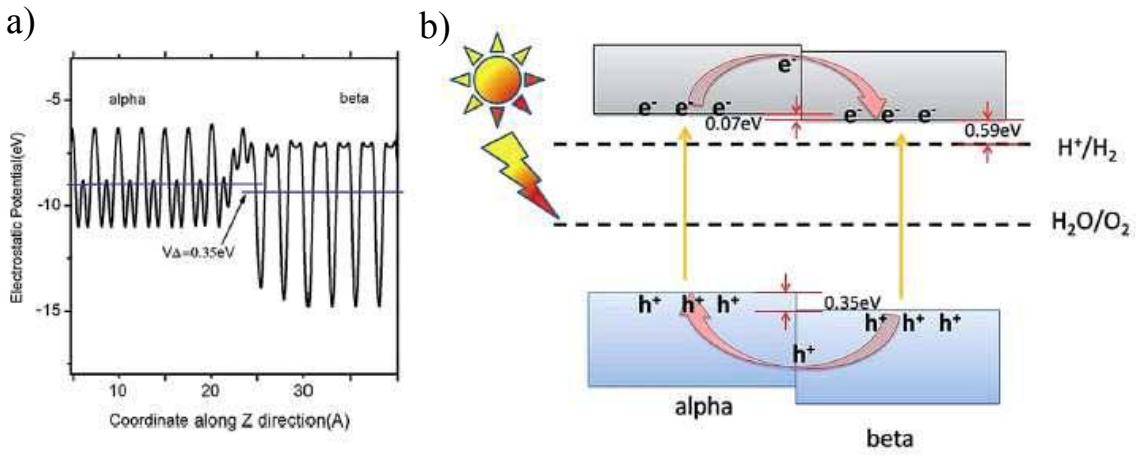

Figure 12. (a) The electronic potential profile for the α-β Ga_2O_3 junction. (b) The schematic illustration of the band-offset in α-β Ga_2O_3 phase-junction. Reprinted with the permission from ref. 100. Copyright 2014 Royal Society of Chemistry.

Other band alignments, including TiO_2-B/anatase and α/β Ga_2O_3 phase-junction, have also been investigated theoretically and experimentally.[99-100] For example, for the α–β Ga_2O_3 phase junction, a first-principles study was performed to reveal the nature of the band alignment and its effect on the efficient separation of photogenerated carriers.[100] It is reported that the strain and lattice misfit at the interface junctions significantly tune their energy bands. Based on the calculation results and the experimentally-observed charge transfer, a type-II band alignment is proposed for α/β Ga_2O_3

phase-junction. This type-II band alignment is with a higher valance band of α-Ga_2O_3 that is 0.35 eV above that of β-Ga_2O_3, and a conduction band offset of only 0.07 eV, as shown in Figure 12. It is suggested that the photogenerated electrons transfer may follow the adiabatic mechanism due to the strong coupling in the conduction bands of two-phase materials.

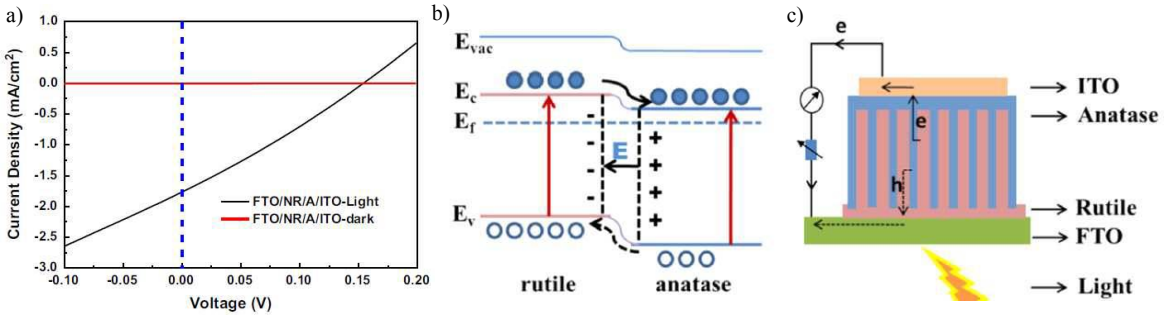

Figure 13. (a) Photocurrent density–voltage (J–V) curve of the photovoltaic device (FTO/rutile/anatase/ITO) under UV illumination. (b) Illustrations of the proposed band alignment of the rutile/anatase coaxial solar cell. (c) Schematic illustration of the TiO_2 phase junction device and the charge carrier transport route. Reprinted with the permission from ref. 101. Copyright 2015 Elsevier.

To demonstrate the band alignment at the interface of phase-junction, a prototype photovoltaic device based on TiO_2 rutile/anatase coaxial nanorod arrays (NRAs) was prepared.[101] Contrasting with photoresist or behavior of single phase TiO_2 devices, the device with anatase-rutile phase-junction shows anordinary photovoltaic response (open-circuit voltage V_{oc}: 154 mV, short-circuit current density J_{sc}: 1.76 mA/cm^2) (Figure 13). These experimental evidences illustrate that the built-in electric field at the interface of anatase-rutile phase-junction in the FTO/rutileNRAs/anatase/ITO device provides the direct driving force for efficient separation of photogenerated charges.

3.2 Time-resolved spectroscopic studies on the promoted charge transfer

The charge transfer process across the phase-junction has been well-studied directly with various techniques.[80, 96, 102-114] With ESR characterizations, the electron transfer from rutile to anatase is claimed in the transition points between anatase and rutile in Degussa P25,[102] while the photoinduced electron transfer from anatase to rutile is proposed in partially reduced P25.[107] With TEM results of the patterned TiO_2(anatase)/TiO_2(rutile) bilayer-type photocatalyst, the interfacial electron transfer from anatase to rutile is explained to be the main reason for the increase of charge separation efficiency, resulting in the high photocatalytic activity of Degussa P25.[115]

Time-resolved spectroscopic techniques, which can characterize the photogenerated charge dynamics directly, have been widely applied in the study of charge transfer across phase-junctions.[112, 116-120] Time-resolved mid-IR spectroscopy, which is proved to be a powerful tool to monitor the photogenerated electron dynamics in semiconductor photocatalyst,[121] is used to study the electron transfer across the phase-junction.[73, 116] Based on the fairly different dynamics of the transient mid-IR absorption in anatase and rutile, the interfacial electron transfer process was analyzed with the relationships between the initial mid-IR absorption and the corresponding phase composition of anatase/rutile phase-junction TiO_2 (Figure 14). The charge transfer process is confirmed across the anatase:rutile phase-junction, and the electron transfer from anatase to rutile is proposed in anatase/rutile TiO_2 prepared by calcination method.

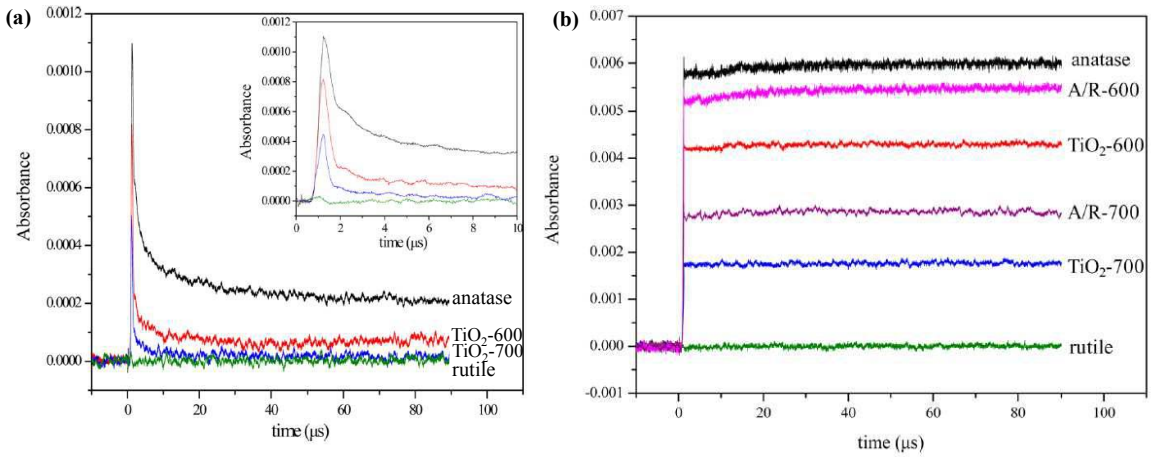

Figure 14. Transient mid-IR absorption decays of pure-phase anatase, pure-phase rutile, and anatase/rutile phase-junction samples of TiO_2-600, TiO_2-700, A/R-600, A/R-700 in vacuum (a) and in 20 Torr of methanol (b) excited by 355 nm laser. The TiO_2-600, TiO_2-700 samples were prepared by calcination method at high temperatures. The A/R-600, A/R-700 TiO_2 samples were mechanically mixed anatase/rutile samples with the same phase compositions of TiO_2-600, TiO_2-700 samples, respectively. Reprinted with permission from Ref. 116. Copyright (2014) American Chemical Society.

By exploiting the different absorption signatures of phtogenerated charges in different phases, transient absorption absorption (TAS) spectroscopy is successfully used to separately track the yield and lifetime of photogenerated charges in different phase sites in the phase-junction composites (Figure 15)[118-119]. The transient absorption signals locate at about 460 and 550 nm are attributed to holes for anatase and rutile TiO_2, respectively. As shown in Figure 15a, it is confirmed that the photogenerated holes transfer from rutile to anatase on submicrosecond time scales, based on the analysis of the spectral shape and position of the absorption signal. On microsecond time scale, the anatase hole yield increase significantly due to the hole transfer, resulting in 5-fold increase for a 20:80 anatase-rutile composite (TiO_2-800). However, the hole transfer does not result in an

increase in charge-carrier lifetime. An intermediate recombination dynamic between that of pure anatase ($t_{1/2} \approx 0.5$ ms) and rutile ($t_{1/2} \approx 20$ms) is obtained in the anatase:rutile junction ($t_{1/2} \approx 4$ ms) (Figure 15c).

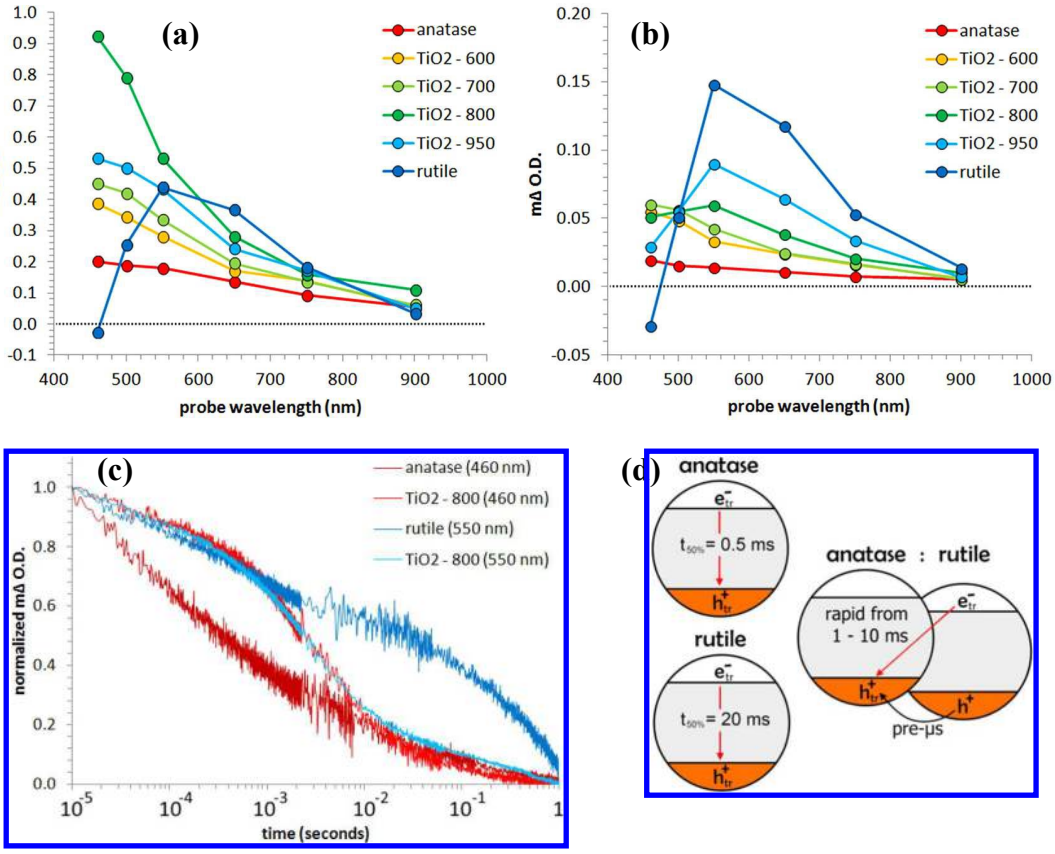

Figure 15. Transient absorption spectra of TiO_2 samples in argon gas atmosphere at (a) 10 μs and (b) 100 ms after a laser pulse (355 nm, 6 ns pulse width). (c) Normalized transient absorption decays in argon gas atmosphere, monitored at 460 nm in anatase and TiO_2-800 and 550 nm in rutile and TiO_2-800 after a laser pulse (355 nm, 6 ns pulse width). Reprinted with permission from Ref. 119. Copyright (2016) American Chemical Society.

Time-resolved photoluminescence spectroscopy, which can reflect the dynamics of photoinduced charges in different phases, is also utilized in the research of the phase-junction roles in solar energy conversion field.[117, 120, 122] Visible (~500 nm) and near-infrared (NIR, ~830 nm)

emission bands were monitored to give insight into the photoinduced charges of anatase and rutile, respectively. New fast photoluminescence decay components appeared in the visible luminescence of rutile-phase dominated TiO_2 and in the NIR luminescence of anatase-rutile phase-junction TiO_2 samples, demonstrating that the charge separation occurred at the phase junction. The charge separation slowed the recombination on the microsecond time scale, while the millisecond decay of the charge carriers in anatase TiO_2 was accelerated with no change in the charge carrier dynamics of rutile TiO_2. Thus, charge separation at the anatase/rutile phase junction caused an increase in the charge carrier concentration on a microsecond time scale, which is likely the main reason for the enhanced photocatalytic activity.

Band alignment and charge separation dynamics across the phase-junction interfaces have been extensively investigated. Since there are multiple types of band alignment at the phase-junction interfaces as discussed for anatase-rutile phase junction in Figure 10, electron migration in either direction between the two phases at the interface has been reported. With transient infrared absorption-excitation energy scanning spectra, Mi et al. claimed that the electron migration direction is controlled by dynamical factors.[80] Thus several strategies are demonstrated to be able to tuning the electron migration direction, such as varying the particle size,[93] putting scavengers on TiO_2 phases, or both. Moreover, the trap-state energetics plays an important role in determining the direction of photogenerated charge separation across phase-junction interfaces.

3.3 Imaging the phase junction

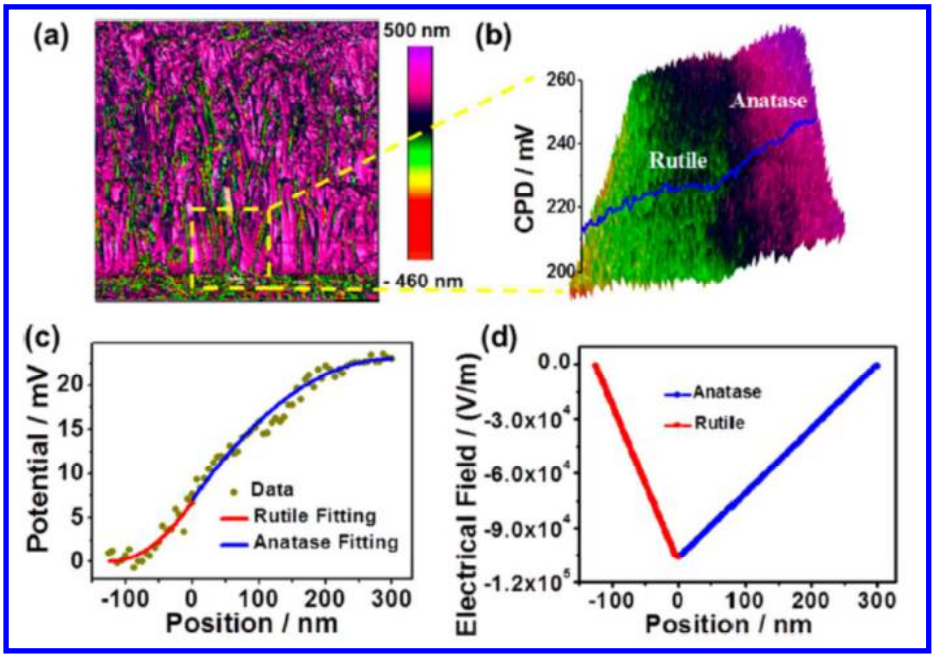

Figure 16. (a) Topographic and (b) 3D surface potential image of the cross section of anatase-rutile phase-junction corresponding to the region as labeled in panel a. (c) The built-in potential distribution of anatase-rutile phase-junction was derived from panel b. (d) The intensity distribution of built-in electric field across the interface of anatase-rutile phase-junction. Reprinted with permission from Ref. 123. Copyright (2017) American Chemical Society.

Microscopy imaging techniques can probe directly the interface structure and their electric properties. Kelvin probe force microscopy (KPFM), which could directly image the local work function of anatase-rutile phase-junction, was employed to measure the surface potential profile across the interface of a model anatase-rutile phase-junction on nanometer scale.[123] The 3D surface potential at the interface of TiO_2 phase junction show obvious difference in surface potential (Figure 16b). Surface potential variation displays gradual change across the interface from rutile to anatase. The CPD of rutile is about 30 mV lower than that of anatase (Figure 16c), demonstrating that work function of rutile is 30 mV higher than that of anatase. An internal built-in electric field up to 1

kV/cm with upward band bending from anatase to rutile was confirmed (Figure 16d). Moreover, the vectorial charge transfer of photogenerated electrons from rutile to anatase was demonstrated with a home-built spatially resolved surface photovoltage spectroscopy (SRSPS) directly.

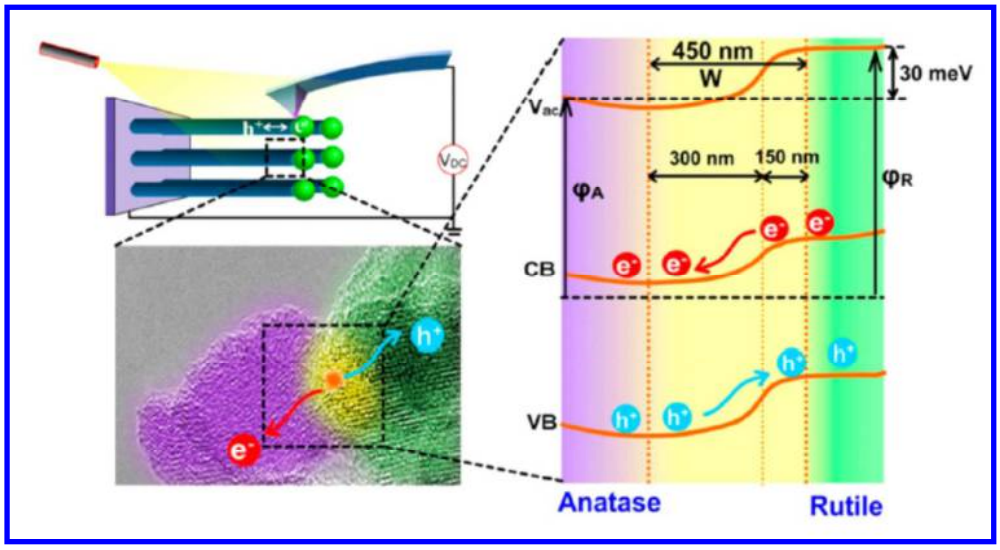

Figure 17. Schematic illustration of obtaining the energy band alignment of a anatase-rutile phase-junction using cross-section KPFM and the transfer direction of photogenerated charges at the interface of a anatase-rutile TiO_2 phase junction. Reprinted with permission from Ref. 123. Copyright (2017) American Chemical Society.

Based on the imaging results, a mechanism for charge separation of anatase-rutile phase-junction is proposed. The surface work function of rutile (φ_R) is higher than that of anatase (φ_A) by 30 mV, indicating that the vacuum energy level of rutile locates above that of anatase. A built-in electric field up to 1 kV/cm is detected at the anatase-rutile phase-junction interface with the direction from anatase toward rutile, demonstrating that the built-in electric field dominates the charge transfer. The direction and strength of built-in electric field should be changed by the synthesis method, doping level, and the lattice alignment across the phase junction, which can in turn affect the charge transfer dynamics.

4. Summary and Perspectives

We have briefly summarized the recent advances in the phase-junction strategy for fabricating internal electric field and promoting charge separation in solar energy conversion filed. The phase junction is more easily formed due to the similar crystal structure between the two phases. The applications of typical phase-junctions, especially anatase-rutile TiO_2 and α-β Ga_2O_3 phase-junction, were reviewed in detail. The anatase-rutile TiO_2 phase-junction has been successfully used in photocatalytic H_2 production and photoelectrochemical water splitting to enhance the activity considerably. The α-β Ga_2O_3 phase-junction improves effectively the photocatalytic performance for the overall water splitting. Then the roles of phase-junction in solar energy conversion were discussed in terms of the band alignment across the phase-junction thermodynamically, and the kinetic mechanism of the phase-junction, from the viewpoint of both time-resolved and spatial resolved characterizations. The built-in electrical field across phase junction is detected directly by the spatial resolved microscopy, and the promoted charge transfer and the retarded charge recombination are characterized separately by time-resolved spectroscopies. It is supposed that the electron migration direction across the phase-junction interface can be controlled by the particle size, the synthesis method, doping level, and the lattice alignment across the phase junction, or the electron/hole scavengers.

To date, the phase-junction used in solar energy conversion is limited to UV-responsive materials, such as TiO_2, Ga_2O_3, et al. To increase the solar energy conversion efficiency, further studies are needed to fabricate phase-junction with visible to near-infrared responsive properties. Doped TiO_2 or visible-responsive semiconductor photocatalyst[124] with various phase structures might be the candidate. With respect to the fundamental understanding of phase-junction, it is

decisive to clarify the controlling factors for direction and strength of the built-in electric field and the direction and efficiency of the charge separation in future. Moreover, the reaction mechanism on different phases for the prepared phase junction, which will determine the performances of the obtained phase-junction, is still an important topic. With continued advances in the fabrication of this diverse family of phase-junction photocatalysts, improved understanding on their kinetic factors, reaction mechanisms, and exploration of new applications, this research field should remain fertile for many years to come.

Acknowledgements

This work was financially supported by 973 National Basic Research Program of the Ministry of Science and Technology (No. 2014CB239400), Strategic Priority Research Program of Chinese Academy of Sciences (No. XDB17000000), and National Natural Science Foundation of China (No. 21633015 and 21621063).

References

(1) Osterloh, F. E. Inorganic Materials as Catalysts for Photochemical Splitting of Water. *Chem. Mater.* **2008**, *20*, 35-54.
(2) Chen, X. B.; Shen, S. H.; Guo, L. J.; Mao, S. S. Semiconductor-Based Photocatalytic Hydrogen Generation. *Chem. Rev.* **2010**, *110*, 6503-6570.
(3) Thompson, Tracy L.; Yates, John T. TiO_2-Based Photocatalysis: Surface Defects, Oxygen and Charge Transfer. *Top. Catal.* **2005**, *35*, 197-210.
(4) Nakata, K.; Fujishima, A. TiO_2 Photocatalysis: Design and Applications. *J. Photochem. Photobiol., C* **2012**, *13*, 169-189.
(5) Fujishima, A.; Zhang, X.; Tryk, D. TiO_2 Photocatalysis and Related Surface Phenomena. *Surf. Sci. Rep.* **2008**, *63*, 515-582.
(6) Xu, H.; Ouyang, S.; Liu, L.; Reunchan, P.; Umezawa, N.; Ye, J. Recent Advances in TiO_2-Based Photocatalysis. *J. Mater. Chem. A* **2014**, *2*, 12642.
(7) Du, H.; Liu, Y. N.; Shen, C. C.; Xu, A. W. Nanoheterostructured Photocatalysts for Improving Photocatalytic Hydrogen Production. *Chin. J. Catal.* **2017**, *38*, 1295-1306.
(8) Wang, H.; Zhang, L.; Chen, Z.; Hu, J.; Li, S.; Wang, Z.; Liu, J.; Wang, X. Semiconductor Heterojunction Photocatalysts: Design, Construction, and Photocatalytic Performances. *Chem. Soc. Rev.* **2014**, *43*, 5234-5244.

(9) Ma, Y.; Wang, X. L.; Li, C. Charge Separation Promoted by Phase Junctions in Titanium Dioxide Photocatalysts. *Chin. J. Catal.* **2015**, *39*, 1519-1527.
(10) Li, R. G.; Li, C. Photocatalytic Water Splitting on Semiconductor-Based Photocatalysts. *Adv. Catal.* **2017**, *60*, 1-57.
(11) Li, R.; Zhang, F.; Wang, D.; Yang, J.; Li, M.; Zhu, J.; Zhou, X.; Han, H.; Li, C. Spatial Separation of Photogenerated Electrons and Holes among {010} and {110} Crystal Facets of $BiVO_4$. *Nat. Commun.* **2013**, *4*, 1432.
(12) Li, R. G.; Han, H. X.; Zhang, F. X.; Wang, D. G.; Li, C. Highly Efficient Photocatalysts Constructed by Rational Assembly of Dual-Cocatalysts Separately on Different Facets of $BiVO_4$. *Energy. Env. Sci.* **2014**, *7*, 1369-1376.
(13) Yamasita, D.; Takata, T.; Hara, M.; Kondo, J. N.; Domen, K. Recent Progress of Visible-Light-Driven Heterogeneous Photocatalysts for Overall Water Splitting. *Solid State Ionics* **2004**, *172*, 591-595.
(14) Yan, H. J.; Yang, J. H.; Ma, G. J.; Wu, G. P.; Zong, X.; Lei, Z. B.; Shi, J. Y.; Li, C. Visible-Light-Driven Hydrogen Production with Extremely High Quantum Efficiency on Pt-PdS/CdS Photocatalyst. *J. Catal.* **2009**, *266*, 165-168.
(15) Yang, J. H.; Wang, D. G.; Han, H. X.; Li, C. Roles of Cocatalysts in Photocatalysis and Photoelectrocatalysis. *Acc. Chem. Res.* **2013**, *46*, 1900-1909.
(16) Zhang, J.; Xu, Q.; Feng, Z.; Li, M.; Li, C. Importance of the Relationship Between Surface Phases and Photocatalytic Activity of TiO_2. *Angew. Chem. Int. Ed.* **2008**, *47*, 1766-1769.
(17) Liu, L.; Zhao, H.; Andino, J. M.; Li, Y. Photocatalytic CO_2 Reduction with H_2O on TiO_2 Nanocrystals: Comparison of Anatase, Rutile, and Brookite Polymorphs and Exploration of Surface Chemistry. *ACS Catal.* **2012**, *2*, 1817-1828.
(18) Hoffmann, M. R.; Martin, S. T.; Choi, W. Y.; Bahnemann, D. W. Environmental Applications of Semiconductor Photocatalysis. *Chem. Rev.* **1995**, *95*, 69-96.
(19) Linsebigler, A. L.; Lu, G. Q.; Yates, J. T. Photocatalysis on TiO_2 Surfaces-Principles, Mechanisms, and Selected Results. *Chem. Rev.* **1995**, *95*, 735-758.
(20) Henderson, M. A. A Surface Science Perspective on TiO_2 Photocatalysis. *Surf. Sci. Rep.* **2011**, *66*, 185-297.
(21) Chen, X.; Mao, S. S. Titanium Dioxide Nanomaterials: Synthesis, Properties, Modifications, and Applications. *Chem. Rev.* **2007**, *107*, 2891-2959.
(22) Pelaez, M.; Nolan, N. T.; Pillai, S. C.; Seery, M. K.; Falaras, P.; Kontos, A. G.; Dunlop, P. S. M.; Hamilton, J. W. J.; Byrne, J. A.; O'Shea, K.; et al. A Review on the Visible Light Active Titanium Dioxide Photocatalysts for Environmental Applications. *Appl. Catal. B-Environ.* **2012**, *125*, 331-349.
(23) Schneider, J.; Matsuoka, M.; Takeuchi, M.; Zhang, J.; Horiuchi, Y.; Anpo, M.; Bahnemann, D. W. Understanding TiO_2 Photocatalysis: Mechanisms and Materials. *Chem. Rev.* **2014**, *114*, 9919-9986.
(24) Ma, Y.; Wang, X. L.; Jia, Y. S.; Chen, X. B.; Han, H. X.; Li, C. Titanium Dioxide-Based Nanomaterials for Photocatalytic Fuel Generations. *Chem. Rev.* **2014**, *114*, 9987-10043.
(25) Ohno, T.; Tokieda, K.; Higashida, S.; Matsumura, M. Synergism Between Rutile and Anatase TiO_2 Particles in Photocatalytic Oxidation of Naphthalene. *Appl. Catal., A* **2003**, *244*, 383-391.
(26) Sun, B.; Smirniotis, P. G. Interaction of Anatase and Rutile TiO_2 Particles in Aqueous Photooxidation. *Catal. Today* **2003**, *88*, 49-59.

(27) Bakardjieva, S.; Šubrt, J.; Štengl, V.; Dianez, M. J.; Sayagues, M. J. Photoactivity of Anatase–Rutile TiO_2 Nanocrystalline Mixtures Obtained by Heat Treatment of Homogeneously Precipitated Anatase. *Appl. Catal. B-Environ.* **2005**, *58*, 193-202.
(28) Yan, M. C.; Chen, F.; Zhang, J. L.; Anpo, M. Preparation of Controllable Crystalline Titania and Study on the Photocatalytic Properties. *J. Phys. Chem. B* **2005**, *109*, 8673-8678.
(29) Jiang, D. L.; Zhang, S. Q.; Zhao, H. J. Photocatalytic Degradation Characteristics of Different Organic Compounds at TiO_2 Nanoporous Film Electrodes with Mixed Anatase/Rutile Phases. *Environ. Sci. Technol.* **2007**, *41*, 303-308.
(30) Kuo, H. L.; Kuo, C. Y.; Liu, C. H.; Chao, J. H.; Lin, C. H. A Highly Active Bi-Crystalline Photocatalyst Consisting of TiO_2(B) Nanotube and Anatase Particle for Producing H_2 Gas from Neat Ethanol. *Catal. Lett.* **2007**, *113*, 7-12.
(31) Liu, Z. Y.; Zhang, X. T.; Nishimoto, S.; Jin, M.; Tryk, D. A.; Murakami, T.; Fujishima, A. Anatase TiO_2 Nanoparticles on Rutile TiO_2 Nanorods: A Heterogeneous Nanostructure Via Layer-by-Layer Assembly. *Langmuir* **2007**, *23*, 10916-10919.
(32) Testino, A.; Bellobono, I. R.; Buscaglia, V.; Canevali, C.; D'Arienzo, M.; Polizzi, S.; Scotti, R.; Morazzoni, F. Optimizing the Photocatalytic Properties of Hydrothermal TiO_2 by the Control of Phase Composition and Particle Morphology. A Systematic Approach. *J. Am. Chem. Soc.* **2007**, *129*, 3564-3575.
(33) Baiju, K. V.; Zachariah, A.; Shukla, S.; Biju, S.; Reddy, M. L. P.; Warrier, K. G. K. Correlating Photoluminescence and Photocatalytic Activity of Mixed-Phase Nanocrystalline Titania. *Catal. Lett.* **2008**, *130*, 130-136.
(34) Lei, S.; Weng, D. Highly Active Mixed-Phase TiO_2 Photocatalysts Fabricated at Low Temperature and the Correlation Between Phase Composition and Photocatalytic Activity. *J. Environ. Sci.-China* **2008**, *20*, 1263-1267.
(35) Lin, C. H.; Chao, J. H.; Liu, C. H.; Chang, J. C.; Wang, F. C. Effect of Calcination Temperature on the Structure of a Pt/TiO_2(B) Nanofiber and Its Photocatalytic Activity in Generating H_2. *Langmuir* **2008**, *24*, 9907-9915.
(36) Scotti, R.; Bellobono, I. R.; Canevali, C.; Cannas, C.; Catti, M.; D'Arienzo, M.; Musinu, A.; Polizzi, S.; Sommariva, M.; Testino, A.; et al. Sol-Gel Pure and Mixed-Phase Titanium Dioxide for Photocatalytic Purposes: Relations Between Phase Composition, Catalytic Activity, and Charge-Trapped Sites. *Chem. Mater.* **2008**, *20*, 4051-4061.
(37) Zhao, L.; Han, M.; Lian, J. Photocatalytic Activity of TiO_2 Films with Mixed Anatase and Rutile Structures Prepared by Pulsed Laser Deposition. *Thin Solid Films* **2008**, *516*, 3394-3398.
(38) Xu, M.; Gao, Y.; Moreno, E. M.; Kunst, M.; Muhler, M.; Wang, Y.; Idriss, H.; Wöll, C. Photocatalytic Activity of Bulk TiO_2 Anatase and Rutile Single Crystals Using Infrared Absorption Spectroscopy. *Phys. Rev. Lett.* **2011**, *106*, 138302.
(39) Bilecka, I.; Barczuk, P. J.; Augustynski, J. Photoanodic Oxidation of Small Organic Molecules at Nanostructured TiO_2 Anatase and Rutile Film Electrodes. *Electrochim. Acta* **2010**, *55*, 979-984.
(40) Maeda, K. Direct Splitting of Pure Water into Hydrogen and Oxygen Using Rutile Titania Powder as a Photocatalyst. *Chem. Commun.* **2013**, *49*, 8404-8406.
(41) Li, R.; Weng, Y.; Zhou, X.; Wang, X. L.; Mi, Y.; Chong, R.; Han, H.; Li, C. Achieving Overall Water Splitting Using Titanium Dioxide-Based Photocatalysts of Different Phases. *Energy. Env. Sci.* **2015**, *8*, 2377-2382.

(42) Xu, Q.; Ma, Y.; Zhang, J.; Wang, X. L.; Feng, Z.; Li, C. Enhancing Hydrogen Production Activity and Suppressing CO Formation from Photocatalytic Biomass Reforming on Pt/ TiO_2 by Optimizing Anatase-Rutile Phase Structure. *J. Catal.* **2011**, *278*, 329-335.
(43) Ma, Y.; Xu, Q.; Chong, R. F.; Li, C. Photocatalytic H_2 Production on TiO_2 with Tuned Phase Structure Via Controlling the Phase Transformation. *J. Mater. Res.* **2013**, *28*, 394-399.
(44) Ma, Y.; Xu, Q.; Zong, X.; Wang, D. G.; Wu, G. P.; Wang, X.; Li, C. Photocatalytic H_2 Production on Pt/TiO_2-SO_4^{2-} with Tuned Surface-Phase Structures: Enhancing Activity and Reducing CO Formation. *Energy. Env. Sci.* **2012**, *5*, 6345-6351.
(45) Wang, H. M.; Tan, X.; Yu, T. Preparation and Photoelectric Property of TiO_2 Nanoparticles Withcontrollable Phase Junctions. *Appl. Surf. Sci.* **2014**, *321*, 531-537.
(46) Wang, Y.; Zhang, J.; Liu, S.Y.; Yan, S.; Wu, W.C.; Xu, Q.; Li, C. Study on the Influence of Ni Modifying on Phase Transformation and Photocatalytic Activity of TiO_2. *China Pet. Process Pe.* **2014**, *16*, 42-49.
(47) Liu, J; Yu, X. L.; Liu, Q. Y.; Liu, R. J.; Shang, X. K.; Zhang, S. S.; Li, W. H.; Zheng, W. Q.; Zhang, G. J.; Cao, H. B.; et al. Surface-Phase Junctions of Branched TiO_2 Nanorod Arrays for Efficient Photoelectrochemical Water Splitting. *Appl. Catal. B* **2014**, *158-159*, 296-300.
(48) Pang, L. X.; Wang, X. Y.; Tang, X. D. Enhanced Photocatalytic Performance of Porous TiO_2 Nanobelts with Phase Junctions. *Solid State Sci.* **2015**, *39*, 39-33.
(49) Zhu, S. C.; Fu, L. Fabricating Rutile Nanopins on an Anatase Hollow Sphere Structure with Enhanced Photoactivity Performance. *Rsc Adv.* **2017**, *7*, 56648-56654.
(50) Yu, Y.; Wen, W.; Qian, X. Y.; Liu, J. B.; Wu, J. M. UV and Visible Light Photocatalytic Activity of Au/ TiO_2 Nanoforests with Anatase/Rutile Phase Junctions and Controlled Au Locations. *Sci. Rep.-Uk* **2017**, *7*, 41253.
(51) Yao, H.; Fu, W.; Liu, L.; Li, X.; Ding, D.; Su, P.; Feng, S.; Yang, H. Hierarchical Photoanode of Rutile TiO_2 Nanorods Coupled with Anatase TiO_2 Nanosheets Array for Photoelectrochemical Application. *J. Alloys Compd.* **2016**, *680*, 206-211.
(52) Wang, W. K.; Chen, J. J.; Zhang, X.; Huang, Y. X.; Li, W. W.; Yu, H. Q. Self-Induced Synthesis of Phase-Junction TiO_2 with a Tailored Rutile to Anatase Ratio Below Phase Transition Temperature. *Sci. Rep.-Uk* **2016**, *6*, 20491.
(53) Tiwari, A.; Mondal, I.; Ghosh, S.; Chattopadhyay, N.; Pal, U. Fabrication of Mixed Phase TiO_2 Heterojunction Nanorods and Their Enhanced Photoactivities. *Phys. Chem. Chem. Phys.* **2016**, *18*, 15260-15268.
(54) An, X.; Hu, C.; Liu, H.; Qu, J. Oxygen Vacancy Mediated Construction of Anatase/Brookite Heterophase Junctions for High-Efficiency Photocatalytic Hydrogen Evolution. *J. Mater. Chem. A* **2017**, *5*, 24989-24994.
(55) Ozawa, T.; Iwasaki, M.; Tada, H.; Akita, T.; Tanaka, K.; Ito, S. Low-Temperature Synthesis of Anatase-Brookite Composite Nanocrystals: The Junction Effect on Photocatalytic Activity. *J. Colloid Interface Sci.* **2005**, *281*, 510-513.
(56) Qiu, Y.; Ouyang, F. Fabrication of TiO_2 Hierarchical Architecture Assembled by Nanowires with Anatase/ TiO_2 (B) Phase-Junctions for Efficient Photocatalytic Hydrogen Production. *Appl. Surf. Sci.* **2017**, *403*, 691-698.
(57) Bai, Y.; Li, W.; Liu, C.; Yang, Z. H.; Feng, X.; Lu, X. H.; Chan, K. Y. Stability of Pt Nanoparticles and Enhanced Photocatalytic Performance in Mesoporous Pt-(Anatase/TiO_2(B)) Nanoarchitecture. *J. Mater. Chem.* **2009**, *19*, 7055-7061.

(58) Liu, B.; Khare, A.; Aydil, E. S. TiO_2-B/Anatase Core-Shell Heterojunction Nanowires for Photocatalysis. *ACS Appl. Mater. Interfaces* **2011**, *3*, 4444-4450.
(59) Mohamed, M. M.; Asghar, B. H. M.; Muathen, H. A. Facile Synthesis of Mesoporous Bicrystallized TiO_2(B)/Anatase (Rutile) Phases as Active Photocatalysts for Nitrate Reduction. *Catal. Commun.* **2012**, *28*, 58-63.
(60) Parayil, S. K.; Kibombo, H. S.; Mahoney, L.; Wu, C. M.; Yoon, M.; Koodali, R. T. Synthesis of Mixed Phase Anatase-TiO_2(B) by a Simple Wet Chemical Method. *Mater. Lett.* **2013**, *95*, 175-177.
(61) Zheng, Z. F.; Liu, H. W.; Ye, J. P.; Zhao, J. C.; Waclawik, E. R.; Zhu, H. Y. Structure and Contribution to Photocatalytic Activity of the Interfaces in Nanofibers with Mixed Anatase and TiO_2(B) Phases. *J. Mol. Catal. A: Chem.* **2010**, *316*, 75-82.
(62) Zhou, W. J.; Gai, L. G.; Hu, P. G.; Cui, J. J.; Liu, X. Y.; Wang, D. Z.; Li, G. H.; Jiang, H. D.; Liu, D.; Liu, H.; et al. Phase Transformation of TiO_2 Nanobelts and TiO_2(B)/Anatase Interface Heterostructure Nanobelts with Enhanced Photocatalytic Activity. *CrystEngComm* **2011**, *13*, 6643-6649.
(63) Dai, J.; Yang, J.; Wang, X.; Zhang, L.; Li, Y. Enhanced Visible-Light Photocatalytic Activity for Selective Oxidation of Amines into Imines over TiO_2(B)/Anatase Mixed-Phase Nanowires. *Appl. Surf. Sci.* **2015**, *349*, 343-352.
(64) An, X.; Hu, C.; Liu, H.; Qu, J. Hierarchical Nanotubular Anatase/Rutile/TiO_2(B) Heterophase Junction with Oxygen Vacancies for Enhanced Photocatalytic H_2 Production. *Langmuir* **2018**, *34*, 1883-1889.
(65) Takahara, I.; Saito, M.; Inaba, M.; Murata, K. Effects of Pre-Treatment of a Silica-Supported Gallium Oxide Catalyst with H_2 on Its Catalytic Performance for Dehydrogenation of Propane. *Catal. Lett.* **2004**, *96*, 29-32.
(66) Zheng, B.; Hua, W. M.; Yue, Y. H.; Gao, Z. Dehydrogenation of Propane to Propene Over Different Polymorphs of Gallium Oxide. *J. Catal.* **2005**, *232*, 143-151.
(67) Hou, Y. D.; Wu, L.; Wang, X. C.; Ding, Z. X.; Li, Z. H.; Fu, X. Z. Photocatalytic Performance of Alpha-, Beta-, and Gamma-Ga_2O_3 for the Destruction of Volatile Aromatic Pollutants in Air. *J. Catal.* **2007**, *250*, 12-18.
(68) Yanagida, T.; Sakata, Y.; Imamura, H. Photocatalytic Decomposition of H_2O into H_2 and O_2 Over Ga_2O_3 Loaded with NiO. *Chem. Lett.* **2004**, *33*, 726-727.
(69) Sakata, Y.; Matsuda, Y.; Yanagida, T.; Hirata, K.; Imamura, H.; Teramura, K. Effect of Metal Ion Addition in a Ni Supported Ga_2O_3 Photocatalyst on the Photocatalytic Overall Splitting of H_2O. *Catal. Lett.* **2008**, *125*, 22-26.
(70) Filippo, E.; Tepore, M.; Baldassarre, F.; Siciliano, T.; Micocci, G.; Quarta, G.; Calcagnile, L.; Tepore, A. Synthesis of Beta-Ga_2O_3 Microstructures with Efficient Photocatalytic Activity by Annealing of Gase Single Crystal. *Appl. Surf. Sci.* **2015**, *338*, 69-74.
(71) Liu, J.; Zhang, G. K. Mesoporous Mixed-Phase Ga_2O_3: Green Synthesis and Enhanced Photocatalytic Activity. *Mater. Res. Bull.* **2015**, *68*, 254-259.
(72) Wang, X.; Xu, Q.; Fan, F.; Wang, X. L.; Li, M.; Feng, Z.; Li, C. Study of the Phase Transformation of Single Particles of Ga_2O_3 by UV-Raman Spectroscopy and High-Resolution TEM. *Chem. Asian J.* **2013**, *8*, 2189-2195.
(73) Wang, X.; Xu, Q.; Li, M.; Shen, S.; Wang, X. L.; Wang, Y.; Feng, Z.; Shi, J.; Han, H.; Li, C. Photocatalytic Overall Water Splitting Promoted by an Alpha-Beta Phase Junction on Ga_2O_3. *Angew. Chem., Int. Ed.* **2012**, *51*, 13089-13092.

(74) Jin, S.; Wang, X.; Wang, X. L.; Ju, M; Shen, S.; Liang, W.; Zhao, Y.; Feng, Z.; Playford, H. Y.; Walton, R. I.; et al. Effect of Phase Junction Structure on the Photocatalytic Performance in Overall Water Splitting: Ga_2O_3 Photocatalyst as an Example. *J. Phys. Chem. C* **2015**, *119*, 18221-18228.
(75) Cao, F.; Xiong, J.; Wu, F.; Liu, Q.; Shi, Z.; Yu, Y.; Wang, X.; Li, L. Enhanced Photoelectrochemical Performance from Rationally Designed Anatase/Rutile Ga_2O_3 Heterostructures. *ACS Appl. Mater. Interfaces* **2016**, *8*, 12239-12245.
(76) Wang, X.; Jin, S.; An, H.; Wang, X. L.; Feng, Z.; Li, C. Relation Between the Photocatalytic and Photoelectrocatalytic Performance for the Particulate Semiconductor-Based Photoconversion Systems with Surface Phase Junction Structure. *J. Phys. Chem. C* **2015**, *119*, 22460-22464.
(77) Li, A.; Wang, Z.; Yin, H.; Wang, S.; Yan, P.; Huang, B.; Wang, X. L.; Li, R.; Zong, X.; Han, H.; et al. Understanding the Anatase–Rutile Phase Junction in Charge Separation and Transfer in a TiO_2 Electrode for Photoelectrochemical Water Splitting. *Chem. Sci.* **2016**, *7*, 6076-6082.
(78) Wang, H.; Tan, X.; Yu, T. Preparation and Photoelectric Property of TiO_2 Nanoparticles with Controllable Phase Junctions. *Appl. Surf. Sci.* **2014**, *321*, 531-537.
(79) Liu, J.; Yu, X.; Liu, Q.; Liu, R.; Shang, X.; Zhang, S.; Li, W.; Zheng, W.; Zhang, G.; Cao, H.; et al. Surface-Phase Junctions of Branched TiO_2 Nanorod Arrays for Efficient Photoelectrochemical Water Splitting. *Appl. Catal. B-Environ.* **2014**, *158-159*, 296-300.
(80) Mi, Y.; Weng, Y. X. Band Alignment and Controllable Electron Migration Between Rutile and Anatase TiO_2. *Sci. Rep.-Uk* **2015**, *5*, 11482.
(81) Deák, P.; Aradi, B.; Frauenheim, T. Band Lineup and Charge Carrier Separation in Mixed Rutile-Anatase Systems. *J. Phys. Chem. C* **2011**, *115*, 3443-3446.
(82) Kang, J.; Wu, F.; Li, S. S.; Xia, J. B.; Li, J. Calculating Band Alignment Between Materials with Different Structures: The Case of Anatase and Rutile Titanium Dioxide. *J. Phys. Chem. C* **2012**, *116*, 20765-20768.
(83) Pfeifer, V.; Erhart, P.; Li, S. Y.; Rachut, K.; Morasch, J.; Brotz, J.; Reckers, P.; Mayer, T.; Ruhle, S.; Zaban, A.; et al. Energy Band Alignment Between Anatase and Rutile TiO_2. *J. Phys. Chem. Lett.* **2013**, *4*, 4182-4187.
(84) Scanlon, D. O.; Dunnill, C. W.; Buckeridge, J.; Shevlin, S. A.; Logsdail, A. J.; Woodley, S. M.; Catlow, C. R.; Powell, M. J.; Palgrave, R. G.; Parkin, I. P.; et al. Band Alignment of Rutile and Anatase TiO_2. *Nat. Mater.* **2013**, *12*, 798-801.
(85) Wang, J.; Liu, X. L.; Yang, A. L.; Zheng, G. L.; Yang, S. Y.; Wei, H. Y.; Zhu, Q. S.; Wang, Z. G. Measurement of Wurtzite ZnO/Rutile TiO_2 Heterojunction Band Offsets by X-Ray Photoelectron Spectroscopy. *Appl. Phys. A* **2010**, *103*, 1099-1103.
(86) Wang, H.; Wu, Z.; Liu, Y.; Sheng, Z. The Characterization of ZnO–Anatase–Rutile Three-Component Semiconductor and Enhanced Photocatalytic Activity of Nitrogen Oxides. *J. Mol. Catal. A: Chem.* **2008**, *287*, 176-181.
(87) Veal, T. D.; King, P. D. C.; Hatfield, S. A.; Bailey, L. R.; McConville, C. F.; Martel, B.; Moreno, J. C.; Frayssinet, E.; Semond, F.; Zúñiga-Pérez, J. Valence Band Offset of the ZnO/AlN Heterojunction Determined by X-Ray Photoemission Spectroscopy. *Appl. Phys. Lett.* **2008**, *93*, 202108.
(88) Xiong, G.; Shao, R.; Droubay, T. C.; Joly, A. G.; Beck, K. M.; Chambers, S. A.; Hess, W. P. Photoemission Electron Microscopy of TiO_2 Anatase Films Embedded with Rutile Nanocrystals. *Adv. Funct. Mater.* **2007**, *17*, 2133-2138.

(89) Kavan, L.; Gratzel, M.; Gilbert, S. E.; Klemenz, C.; Scheel, H. J. Electrochemical and Photoelectrochemical Investigation of Single-Crystal Anatase. *J. Am. Chem. Soc.* **1996**, *118*, 6716-6723.
(90) Kraut, E.; Grant, R.; Waldrop, J.; Kowalczyk, S. Semiconductor Core-Level to Valence-Band Maximum Binding-Energy Differences: Precise Determination by X-Ray Photoelectron Spectroscopy. *Phys. Rev. B* **1983**, *28*, 1965-1977.
(91) Zhang, Y. Y; Lang, L.; Gu, H. J.; Chen, S.; Liu, Z. P.; Xiang, H.; Gong, X. G. Origin of the Type-II Band Offset Between Rutile and Anatase Titanium Dioxide: Classical and Quantum-Mechanical Interactions Between O Ions. *Phys. Rev. B* **2017**, *95*, 155308.
(92) Conesa, J. C. Modeling with Hybrid Density Functional Theory the Electronic Band Alignment at the Zinc Oxide–Anatase Interface. *J. Phys. Chem. C* **2012**, *116*, 18884-18890.
(93) Ko, K. C.; Bromley, S. T.; Lee, J. Y.; Illas, F. Size-Dependent Level Alignment Between Rutile and Anatase TiO_2 Nanoparticles: Implications for Photocatalysis. *J. Phys. Chem. Lett.* **2017**, *8*, 5593-5598.
(94) Kho, Y. K.; Iwase, A.; Teoh, W. Y.; Madler, L.; Kudo, A.; Amal, R. Photocatalytic H_2 Evolution Over TiO_2 Nanoparticles. The Synergistic Effect of Anatase and Rutile. *J. Phys. Chem. C* **2010**, *114*, 2821-2829.
(95) Knorr, F. J.; Mercado, C. C.; McHale, J. L. Trap-State Distributions and Carrier Transport in Pure and Mixed-Phase TiO_2: Influence of Contacting Solvent and Interphasial Electron Transfer. *J. Phys. Chem. C* **2008**, *112*, 12786-12794.
(96) Hurum, D. C.; Agrios, A. G.; Crist, S. E.; Gray, K. A.; Rajh, T.; Thurnauer, M. C. Probing Reaction Mechanisms in Mixed Phase TiO_2 by EPR. *J. Electron Spectrosc. Relat. Phenom.* **2006**, *150*, 155-163.
(97) Zhu, S. C.; Xie, S. H.; Liu, Z. P. Nature of Rutile Nuclei in Anatase-to-Rutile Phase Transition. *J. Am. Chem. Soc.* **2015**, *137*, 11532–11539.
(98) Zhao, W. N.; Zhu, S. C.; Li, Y. F.; Liu, Z. P. Three-Phase Junction for Modulating Electron-Hole Migration in Anatase-Rutile Photocatalysts. *Chem. Sci.* **2015**, *6*, 3483-3494.
(99) Zhu, S. C.; Xie, S. H.; Liu, Z. P. Design and Observation of Biphase TiO_2 Crystal with Perfect Junction. *J. Phys. Chem. Lett.* **2014**, *5*, 3162-3168.
(100) Ju, M. G.; Wang, X.; Liang, W. Z.; Zhao, Y.; Li, C. Tuning the Energy Band-Gap of Crystalline Gallium Oxide to Enhance Photocatalytic Water Splitting: Mixed-Phase Junctions. *J. Mater. Chem. A* **2014**, *2*, 17005-17014.
(101) Yan, P.; Wang, X.; Zheng, X.; Li, R.; Han, J.; Shi, J.; Li, A.; Gan, Y.; Li, C. Photovoltaic Device Based on TiO_2 Rutile/Anatase Phase Junctions Fabricated in Coaxial Nanorod Arrays. *Nano Energy* **2015**, *15*, 406-412.
(102) Hurum, D. C.; Agrios, A. G.; Gray, K. A.; Rajh, T.; Thurnauer, M. C. Explaining the Enhanced Photocatalytic Activity of Degussa P25 Mixed-Phase TiO_2 Using EPR. *J. Phys. Chem. B* **2003**, *107*, 4545-4549.
(103) Hurum, D. C.; Gray, K. A.; Rajh, T.; Thurnauer, M. C. Photoinitiated Reactions of 2,4,6 TCP on Degussa P25 Formulation TiO_2: Wavelength-Sensitive Decomposition. *J. Phys. Chem. B* **2004**, *108*, 16483-16487.
(104) Skryshevskyy, V. A.; Dittrich, Th; Rappich, J. Infrared–Active Defects in a TiO_2 Mixture of Coexisting Anatase and Rutile Phases. *Phys. Status Solidi A* **2004**, *201*, 157-161.

(105) Hurum, D. C.; Gray, K. A.; Rajh, T.; Thurnauer, M. C. Recombination Pathways in the Degussa P25 Formulation of TiO_2: Surface Versus Lattice Mechanisms. *J. Phys. Chem. B* **2005**, *109*, 977-980.

(106) Nakajima, H.; Mori, T.; Shen, Q.; Toyoda, T. Photoluminescence Study of Mixtures of Anatase and Rutile TiO_2 Nanoparticles: Influence of Charge Transfer Between the Nanoparticles on Their Photoluminescence Excitation Bands. *Chem. Phys. Lett.* **2005**, *409*, 81-84.

(107) Komaguchi, K.; Nakano, H.; Araki, A.; Harima, Y., Photoinduced Electron Transfer from Anatase to Rutile in Partially Reduced TiO_2(P25) Nanoparticles: An ESR Study. *Chem. Phys. Lett.* **2006**, *428*, 338-342.

(108) Shen, Q.; Katayama, K.; Sawada, T.; Yamaguchi, M.; Kumagai, Y.; Toyoda, T. Photoexcited Hole Dynamics in TiO_2 Nanocrystalline Films Characterized Using a Lens-Free Heterodyne Detection Transient Grating Technique. *Chem. Phys. Lett.* **2006**, *419*, 464-468.

(109) Wu, Q.; Li, D.; Hou, Y.; Wu, L.; Fu, X.; Wang, X. Study of Relationship between Surface Transient Photoconductivity and Liquid-Phase Photocatalytic Activity of Titanium Dioxide. *Mater. Chem. Phys.* **2007**, *102*, 53-59.

(110) Jing, L.; Li, S.; Song, S.; Xue, L.; Fu, H. Investigation on the Electron Transfer Between Anatase and Rutile in Nano-Sized TiO_2 by Means of Surface Photovoltage Technique and Its Effects on the Photocatalytic Activity. *Sol. Energy Mater. Sol. Cells* **2008**, *92*, 1030-1036.

(111) Li, G.; Richter, C. P.; Milot, R. L.; Cai, L.; Schmuttenmaer, C. A.; Crabtree, R. H.; Brudvig, G. W.; Batista, V. S. Synergistic Effect Between Anatase and Rutile TiO_2 Nanoparticles in Dye-Sensitized Solar Cells. *Dalton Trans.* **2009**, 10078-10085.

(112) Carneiro, J. T.; Savenije, T. J.; Moulijn, J. A.; Mul, G. How Phase Composition Influences Optoelectronic and Photocatalytic Properties of TiO_2. *J. Phys. Chem. C* **2011**, *115*, 2211-2217.

(113) Zhang, X.; Lin, Y.; He, D.; Zhang, J.; Fan, Z.; Xie, T. Interface Junction at Anatase/Rutile in Mixed-Phase TiO_2: Formation and Photo-Generated Charge Carriers Properties. *Chem. Phys. Lett.* **2011**, *504*, 71-75.

(114) Sun, X.; Dai, W.; Wu, G.; Li, L.; Guan, N.; Hunger, M. Evidence of Rutile-to-Anatase Photo-Induced Electron Transfer in Mixed-Phase TiO_2 by Solid-State NMR Spectroscopy. *Chem. Commun.* **2015**, *51*, 13779-13782.

(115) Kawahara, T.; Konishi, Y.; Tada, H.; Tohge, N.; Nishii, J.; Ito, S. A Patterned TiO_2(Anatase)/TiO_2(Rutile) Bilayer-Type Photocatalyst: Effect of the Anatase/Rutile Junction on the Photocatalytic Activity. *Angew. Chem. Int. Edit.* **2002**, *41*, 2811-2813.

(116) Shen, S.; Wang, X. L.; Chen, T.; Feng, Z.; Li, C. Transfer of Photoinduced Electrons in Anatase-Rutile TiO_2 Determined by Time Resolved Mid-Infrared Spectroscopy. *J. Phys. Chem. C* **2014**, *118*, 12661-12668.

(117) Wang, X. L.; Feng, Z.; Shi, J.; Jia, G.; Shen, S.; Zhou, J.; Li, C. Trap States and Carrier Dynamics of TiO_2 Studied by Photoluminescence Spectroscopy under Weak Excitation Condition. *Phys. Chem. Chem. Phys.* **2010**, *12*, 7083-7090.

(118) Wang, X. L.; Kafizas, A.; Li, X.; Moniz, S. J. A.; Reardon, P. J. T.; Tang, J.; Parkin, I. P.; Durrant, J. R. Transient Absorption Spectroscopy of Anatase and Rutile: The Impact of Morphology and Phase on Photocatalytic Activity. *J. Phys. Chem. C* **2015**, *119*, 10439-10447.

(119) Kafizas, A.; Wang, X. L.; Pendlebury, S. R.; Barnes, P.; Ling, M.; Sotelo-Vazquez, C.; Quesada-Cabrera, R.; Li, C.; Parkin, I. P.; Durrant, J. R. Where Do Photogenerated Holes Go in

Anatase:Rutile TiO_2? A Transient Absorption Spectroscopy Study of Charge Transfer and Lifetime. *J. Phys. Chem. A* **2016**, *120*, 715-723.

(120) Wang, X. L.; Shen, S.; Feng, Z.; Li, C. Time-Resolved Photoluminescence of Anatase/Rutile TiO_2 Phase Junction Revealing Charge Separation Dynamics. *Chin. J. Catal.* **2016**, *37*, 2059-2068.

(121) Chen, T.; Feng, Z. H.; Wu, G. P.; Shi, J. Y.; Ma, G. J.; Ying, P. L.; Li, C. Mechanistic Studies of Photocatalytic Reaction of Methanol for Hydrogen Production on Pt/TiO_2 by in Situ Fourier Transform IR and Time-Resolved IR Spectroscopy. *J. Phys. Chem. C* **2007**, *111*, 8005-8014.

(122) Shi, J.; Chen, J.; Feng, Z.; Chen, T.; Lian, Y.; Wang, X. L.; Li, C. Photoluminescence Characteristics of TiO_2 and Their Relationship to the Photoassisted Reaction of Water/Methanol Mixture. *J. Phys. Chem. C* **2007**, *111*, 693-699.

(123) Gao, Y.; Zhu, J.; An, H.; Yan, P.; Huang, B.; Chen, R.; Fan, F.; Li, C. Directly Probing Charge Separation at Interface of TiO_2 Phase Junction. *J. Phys. Chem. Lett.* **2017**, *8*, 1419-1423.

(124) Lv, C.; Chen, G.; Sun, J.; Zhou, Y. Construction of Alpha-Beta Phase Junction on $Bi_4V_2O_{11}$ Via Electrospinning Retardation Effect and Its Promoted Photocatalytic Performance. *Inorg. Chem.* **2016**, *55*, 4782-4789.

TOC Graphic

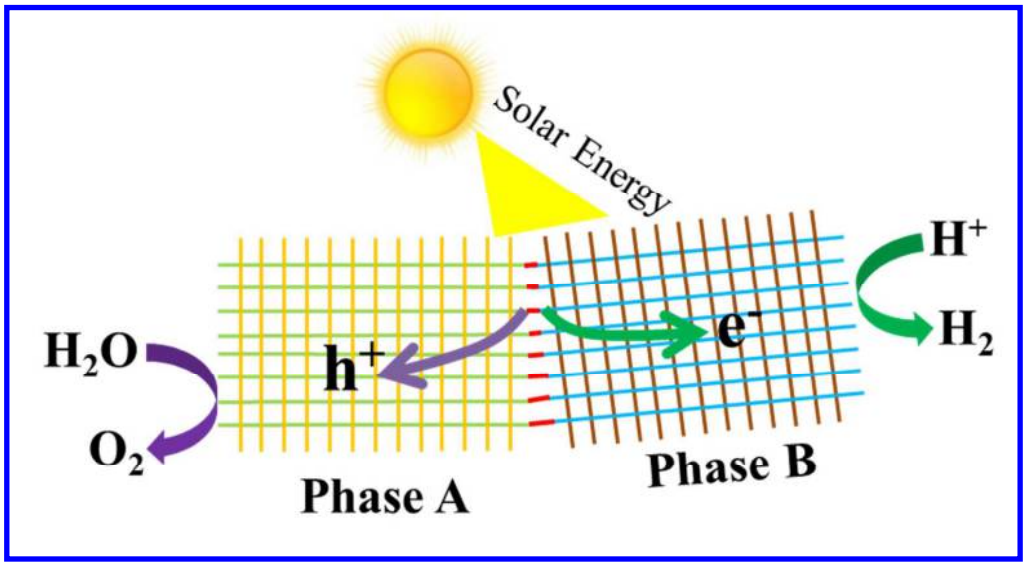

Biographies

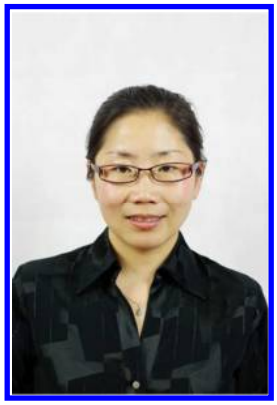

Xiuli Wang is an Associate Professor in Dalian Institute of Chemical Physics (DICP), Chinese Academy of Sciences, China. She obtained a B.Sc. degree in Chemistry from Nankai University (2004) and a Ph.D. degree in Physical Chemistry from DICP (2011). She did postdoctoral research at Imperial College London (2012-2013). Her research interests include time-resolved spectroscopic study on photoinduced charge dynamics, interfacial charge transfer, and mechanism and kinetics of surface reactions in solar fuel production and solar cell.

Can Li received a Ph.D. degree in Physical Chemistry from Dalian Institute of Chemical Physics, Chinese Academy of Sciences in 1989, and he joined the same institute and was promoted to full professor in 1993. He did postdoctoral research at Northwestern University and was a visiting professor at Lehigh University, the University of Liverpool, and the Queensland University, and he was awarded the JSPS Professor at Waseda University, Tokyo University of Technology, and Hokkaido University. He was an invited professor at Université Pierreet Marie Curie, Paris VI. He was the President of the International Association of Catalysis Societies (2008-2012). Currently, he is the director of Dalian National Laboratory for Clean Energy. His research interests are (1) UV Raman spectroscopy and ultrafast spectroscopy; (2) environmental catalysis and green catalysis; (3) heterogeneous asymmetric catalysis; and (4) solar energy conversion and utilization.